Journal of Medicinal Chemistry

Article

pubs.acs.org/jmc

Discovery of 4-{4-[(3*R*)-3-Methylmorpholin-4-yl]-6-[1-(methylsulfonyl)cyclopropyl]pyrimidin-2-yl}-1*H*-indole (AZ20): A Potent and Selective Inhibitor of ATR Protein Kinase with Monotherapy in Vivo Antitumor Activity

Kevin M. Foote,*[,†] Kevin Blades,[†] Anna Cronin,[†] Shaun Fillery,[†] Sylvie S. Guichard,[†] Lorraine Hassall,[†] Ian Hickson,[‡] Xavier Jacq,[‡] Philip J. Jewsbury,[†] Thomas M. McGuire,[†] J. Willem M. Nissink,[†] Rajesh Odedra,[†] Ken Page,[†] Paula Perkins,[†] Abid Suleman,[†] Kin Tam,[†] Pia Thommes,[†] Rebecca Broadhurst,[†] and Christine Wood[†]

[†]AstraZeneca, Mereside, Alderley Park, Macclesfield, Cheshire SK10 4TG, U.K.

[‡]KuDOS Pharmaceuticals, Cambridge Science Park, Milton Road, Cambridge, U.K.

Supporting Information

ABSTRACT: ATR is an attractive new anticancer drug target whose inhibitors have potential as chemo- or radiation sensitizers or as monotherapy in tumors addicted to particular DNA-repair pathways. We describe the discovery and synthesis of a series of sulfonylmorpholinopyrimidines that show potent and selective ATR inhibition. Optimization from a high quality screening hit within tight SAR space led to compound **6** (AZ20) which inhibits ATR immunoprecipitated from HeLa nuclear extracts with an IC_{50} of 5 nM and ATR mediated phosphorylation of Chk1 in HT29 colorectal adenocarcinoma tumor cells with an IC_{50} of 50 nM. Compound **6** potently inhibits the growth of LoVo colorectal adenocarcinoma tumor cells in vitro and has high free exposure in mouse following moderate oral doses. At well tolerated doses **6** leads to significant growth inhibition of LoVo xenografts grown in nude mice. Compound **6** is a useful compound to explore ATR pharmacology in vivo.

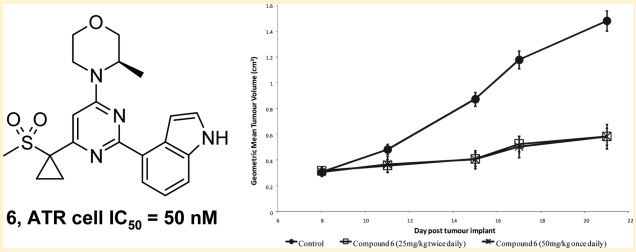

INTRODUCTION

Ataxia telangiectasia mutated and RAD3-related (ATR) is a serine/threonine protein kinase that, together with ATM and DNA-PK, forms part of the DNA-damage response (DDR) coordinating the cellular response to DNA damage, stress, and cell-cycle perturbation.[1] ATR is essential to the viability of replicating cells responding to accumulation of single strand breaks (SSB) in DNA such as stalled replication forks and to bulky DNA damage lesions such as those formed by chemotherapeutics and ultraviolet (UV) radiation.[2−4] Sensitization of tumor cells to chemotherapeutic agents has been demonstrated following genetic modulation of ATR activity,[5] with weak ATR inhibitors such as caffeine,[6,7] and more recently with potent and selective ATR inhibitors such as VE-821.[8,9] These studies suggest that combination of ATR inhibitors with some cytotoxic agents may be therapeutically beneficial. A further compelling utility is aligned with the concept of synthetic lethality.[10] Tumor cells that are deficient in G1 checkpoint controls, in particular p-53, or with other mutations that promote replicative stress, are hypothesized to be more reliant on ATR for survival.[11] In such circumstances, specific inhibition of ATR may lead to enhanced antitumor activity while minimizing normal tissue toxicity. In summary, ATR is an important new drug target whose inhibitors have the potential for broad utility in cancer patients as monotherapy or in combination with chemo- or radiotherapy.

ATR, ATM, and DNA-PK together with three other proteins mTOR, hSMG-1, and TRRAP are members of an atypical class of protein kinases known collectively as the phosphatidylinositol 3-kinase related kinase (PIKK) family. These proteins are structurally different from classical protein kinases and are more closely related to the PI3-kinase family of phospholipid kinases.[12,13] A number of compounds are known to inhibit the PIKK family, which have recently been reviewed elsewhere.[13] One of the first potent PIKK-family inhibitors to be described was **1** (LY294002, Figure 1). Compound **1** inhibits PI3K, mTOR, and DNA-PK and was shown, through X-ray crystallography in complex with PI3Kγ, to make a crucial hydrogen bond interaction to the ATP-binding domain through the morpholine oxygen.[14] Identification of the morpholine hinge binding motif has led to a number of other inhibitors of the PIKK family including ATM, DNA-PK, PI3K, and mTOR, some of which have reached human trials.[15] One such compound is the pan-PI3K inhibitor **2** (GDC-0941), which is currently in phase II trials for the treatment of non-small-cell

Received: December 17, 2012
Published: February 11, 2013

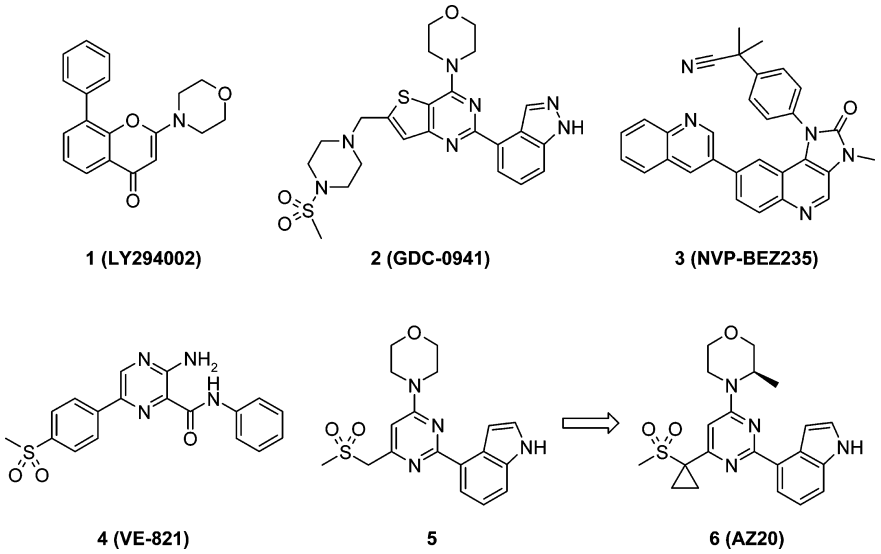

Figure 1. Example PIKK family and ATR inhibitors.

lung cancer.[15a] However, there are few reports describing potent and selective inhibitors of ATR. Compound **3** (NVP-BEZ235), originally described as a dual PI3K and mTOR inhibitor,[16] has also been shown to inhibit DNA-PK, ATM, and ATR.[17,18] Recently, however, scientists at Vertex have described a series 3-amino-6-arylpyrazines such as **4** (VE-821).[8,9] Compound **4** is a potent and selective inhibitor of ATR which potentiates the in vitro cytotoxicity of ionizing radiation (IR) and cisplatin in HCT116 colorectal cancer cells.

Despite the recently described advances in the identification of potent ATR inhibitors such as **4**, a need exists to identify inhibitors suitable for exploring the complex biology of ATR-mediated DNA repair in vivo and of high enough quality to enter human clinical trials. In this report, we describe our early discovery efforts starting from the mTOR-derived screening hit **5**,[15d] which led to the discovery of compound **6** (AZ20).[19] Compound **6** shows monotherapy in vivo antitumor efficacy in LoVo colorectal xenografts in nude mice and is a useful compound for further studies.

CHEMISTRY

Compounds were prepared as shown in Schemes 1−4. Test compounds were synthesized via Suzuki cross-coupling either from 2-chloropyrimidine intermediates (Scheme 2, compounds **62** and **66**−**78**) or from 2-thiomethyl substituted pyrimidines (Scheme 3, compounds **84** and **85**) with the appropriate arylboronic acid or ester.[20] The aryl boronate coupling partners were either commercially available or made from the corresponding aryl bromide or triflate using standard literature methods.[21] The iodomethyl compounds **50**−**52** (Scheme 1) proved to be versatile intermediates allowing variation of the side chain sulfone group and the aryl substituent at position 2 of the pyrimidine ring. Compounds **50**−**52** were prepared starting with a careful substitution of the 4-chloro leaving group in **43** with the appropriate morpholine followed by full reduction of the ester to give the alcohols **47**−**49** and finally iodination. The methylene sulfone unit was elaborated either by direct reaction of the iodomethyl group in **50**−**52** with a sulfinic acid to give **56**−**59** or via the thioethers **64** and **65** followed by oxidation to sulfones **60** and **61**, respectively (Scheme 2). Alternatively, the methylene sulfone moiety can be

Scheme 1[a]

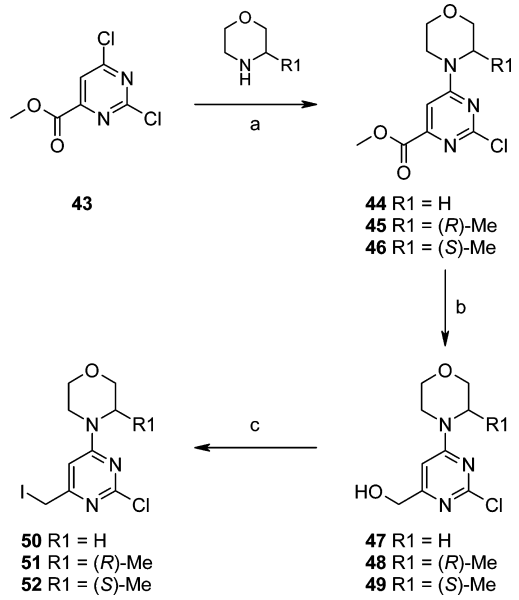

[a]Reagents: (a) Et_3N, DCM, 0 °C → rt; (b) $LiBH_4$, THF, 0 °C → rt; (c) $MeSO_2Cl$, Et_3N, DCM, 0 °C → rt; LiI, acetone, rt or dioxane, 100 °C.

incorporated before the morpholine; compounds **54** and **55** were made starting from the pyrimidinedione **53** by displacement of the chloro leaving group either directly with methanesulfinate to give **54** or first with isopropanethiol followed by full chlorination and then oxidation of sulfide to sulfone to give **55**. Again, careful reaction of the 4-chloro leaving group with morpholine led to **62** and **63**. Alkylation of the methylene unit in intermediates **56**−**63** was carried out using methods such as sodium *tert*-butoxide and MeI in DMF to give **66** or by phase transfer catalysis using TBAB and concentrated NaOH solution in toluene with the appropriate alkylating agent to give the cyclic precursors **67**, **68**, and **71**−**78** (Scheme 2); standard functional group manipulation of the benzyl protecting group in **68** gave **69** and **70**. The 2-SMe substituted pyrimidine precursors **84** and **85** were made from

dx.doi.org/10.1021/jm301859s | J. Med. Chem. 2013, 56, 2125−2138

Scheme 2[a]

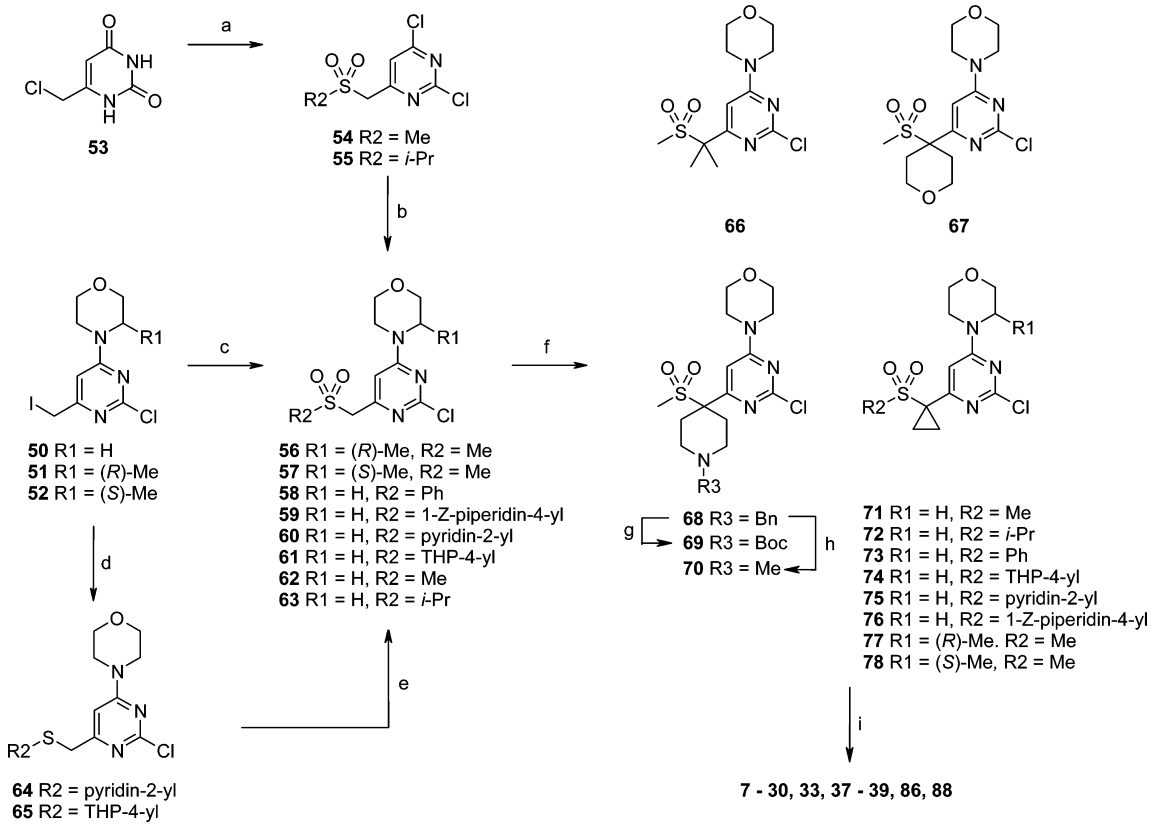

[a]Reagents: (a) compound **54**: NaOS(O)Me, DMF, 125 °C, $POCl_3$, reflux; compound **55**: isopropanethiol, DBU, MeCN, rt, $POCl_3$, reflux, *m*CPBA, DCM, rt; (b) Et_3N, DCM, morpholine, 0 °C → rt; (c) compounds **56** and **57**: NaOS(O)Me, DMF, rt; compound **58**: NaOS(O)Ph, MeCN, 80 °C; compound **59**: sodium 1-*Z*-piperidin-4-ylsulfinate, DMF, rt; (d) *N*,*N*-Diisopropylethylamine, R_2SH, DMF or MeCN, rt; (e) *m*CPBA, DCM, rt; (f) compound **66**: MeI, NaO-*t*-Bu, DMF, 0 °C → rt; compound **67**: 1-bromo-2-(2-bromoethoxy)ethane, 50% aq NaOH, TBAB, DCM, rt; compound **68**: *N*-benzyl-2-chloro-*N*-(2-chloroethyl)ethanamine hydrochloride, NaH, TBAB, NMP, rt → 80 °C; compounds **71**−**78**: 50% aq NaOH, 1,2-dibromoethane, TBAB, toluene, 60 °C or DCM, 30 °C; (g) 1-Chloroethylcarbonochloridate, DCM, rt → reflux, MeOH, di-*tert*-butyl dicarbonate, *N*,*N*-diisopropylethylamine, rt; (h) 1-chloroethylcarbonochloridate, DCM, rt → reflux; $NaBH(OAc)_3$, aq HCHO, $MeCO_2H$, DCM, rt; (i) $Pd_2(Ph_3P)_2Cl_2$, aq Na_2CO_3, indole boronic acid/ester, 18% DMF in 7:3:2 DME/water/EtOH or 4:1 DME/water, microwave/Δ, 90−110 °C; $Pd_2(dba)_3$, tricyclohexylphosphine, KOAc, bis(pinacolato)diboron, bromoindole, dioxane, 100 °C followed by substrate, $Pd(Ph_3P)_4$, aq Na_2CO_3, 100 °C; 1,1′-bis(diphenylphosphine)ferrocene$PdCl_2$, indole triflate, bis(pinacolato)diboron, KOAc, dioxane, 90 °C followed by substrate, $Pd(Ph_3P)_4$, aq Na_2CO_3, 90 °C.

an analogous cyclopropanation procedure from the methylene sulfones **82** and **83** (Scheme 3). Intermediates **82** and **83** were constructed either from **81**[15d] or by reaction of symmetrical dichloropyrimidine **79** with methyl 2-(methylsulfonyl)acetate to give **80** followed by morpholine displacement and decarboxylation. Finally, compounds **31**, **32**, **34**−**36** were prepared by standard functional group manipulation starting from the esters **86** and **88** (Scheme 4).

RESULTS AND DISCUSSION

A directed subset of the AstraZeneca compound collection was screened against ATR in single-shot format at fixed concentrations of 1, 10, and/or 30 μM. As follow-up, the set of actives were filtered stringently based on consensus of inhibition data at the different concentrations and prioritized further using ligand efficiency and, where available, PIKK-family selectivity information. Both screening and dose response follow-up were performed in an ELISA format utilizing ATR immunoprecipitated from HeLa nuclear extracts. A further selection of actives from the screen was assessed for cellular inhibition of ATR kinase activity.

Modest ATR potency was observed across various structural classes of compounds, but a single compound stood out in terms of both potency and selectivity for ATR. Compound **5** is a sulfonylmorpholinopyrimidine from a previously described series inhibiting mammalian target of rapamycin (mTOR) from AstraZeneca[15d] and exhibited high ATR enzyme potency and ligand efficiency (LE) (Table 1). Compound **5** is moderately lipophilic (log $D_{7.4}$ = 1.7) and shows high selectivity against other PIKK and PI3K enzymes. Moreover, compound **5** inhibited ATR-driven phosphorylation of Chk1 at serine-345, a downstream substrate of ATR, following addition of 4-nitroquinoline 1-oxide (4NQO mimics DNA damage caused by UV radiation).[22] ATR cellular IC_{50} was established in an ArrayScan format assay in HT29 colorectal adenocarcinoma cells. The IC_{50} of **5** was 1.1 μM in this assay, which compared favorably with inhibition of mTOR/PI3K-driven phosphorylation of AKT at serine-473 measured in MDA-MB-468 cells (Table 1). Given this profile, compound **5** was an excellent start point from which to develop more potent ATR inhibitors.

On the basis of knowledge from known PIKK inhibitors such as **1**, compound **5** was likely to bind to ATR through the weak morpholine oxygen hydrogen bond acceptor.[14,15] This

dx.doi.org/10.1021/jm301859s | J. Med. Chem. 2013, 56, 2125−2138

Scheme 3[a]

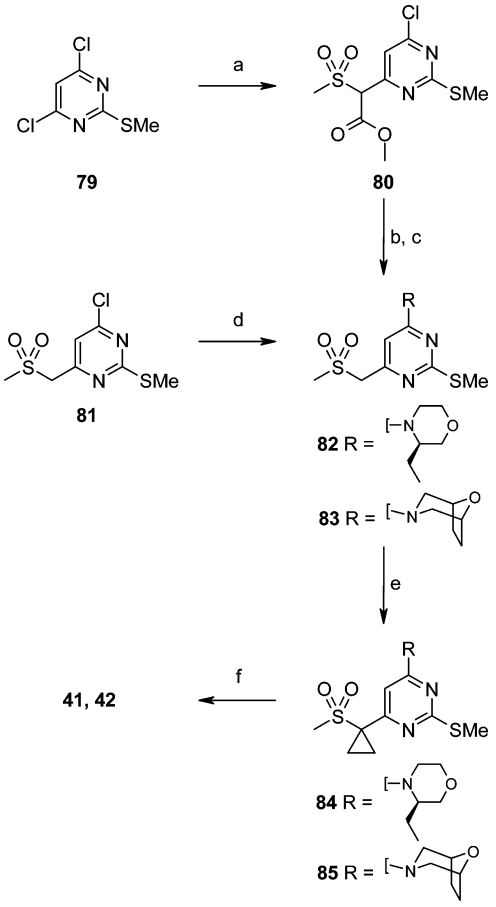

[a]Reagents: (a) methyl 2-(methylsulfonyl)acetate, NaH, DMF, rt; (b) morpholine, *N*,*N*-diisopropylethylamine, DMF, 80 °C; (c) NaOH, MeOH, H_2O, 60 °C; 2 M HCl; (d) morpholine, *N*,*N*-diisopropylethylamine, DCM, rt; (e) NaH, 1,2-dibromoethane, DMF, rt or 50% aq NaOH, 1,2-dibromoethane, TBAB, toluene, 60 °C; (f) $Pd_2(dba)_3$ or $Pd(Ph_3P)_4$, 1*H*-indol-4-ylboronic acid, trifuran-2-ylphosphine, (thiophene-2-carbonyloxy)copper, THF or dioxane, 80 °C.

Scheme 4[a]

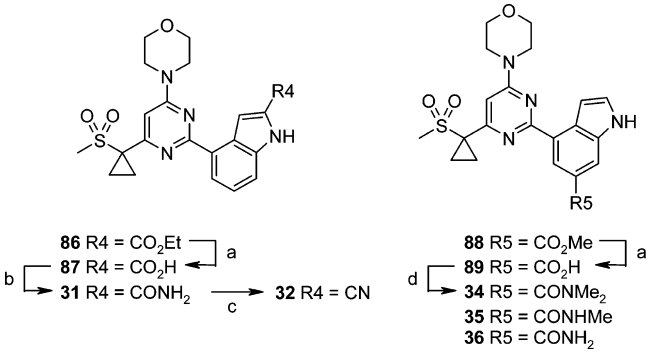

[a]Reagents: (a) LiOH.H_2O, THF, H_2O, rt → 70 °C; (b) HATU, *N*,*N*-diisopropylethylamine, DMF, rt; NH_4Cl, rt; (c) trifluoroacetic anhydride, pyridine, dioxane, 0 °C → rt; (d) HATU, *N*,*N*-diisopropylethylamine, DMF, rt; amine, rt.

hypothesis was supported by attempts to substitute the morpholine for other saturated six-membered-ring heterocyclic groups lacking the hydrogen-bond acceptor oxygen, e.g., piperidine, which resulted in the loss of kinase inhibitory activity. The modeled binding mode of compound **5** in an ATR protein homology model based on the PI3Kγ-isoform offered a tentative explanation of the selectivity for ATR, although a full explanation of selectivity across the PI3K and PIKKs remains elusive (Figure 2). The indole N−H group in **5** likely forms a water-mediated hydrogen bond to Asp2335. Although it is positioned in the binding pocket in a largely similar fashion to PI3K and PIKK targets, we hypothesize that ATR inhibitors from this sulfonylmorpholinopyrimidine series bind slightly deeper into the back pocket. Modeling of the P-loop of the ATR protein suggests further that this region differs from PI3K isoforms, and this may explain in part the selectivity of ATR inhibitors with regard to these targets. Inspection of the model highlighted space for substitution around the methylsulfone region to explore by further compound synthesis, though it was less clear what the impact of such changes would be on selectivity.

Both the presence and position of the indole N−H hydrogen-bond donor group were found to be critical for inhibition of ATR. We were able to test some of the other positional isomers of the indole in **5** with compounds from the AstraZeneca compound collection (Table 2, compounds **7** and **8**). In contrast to mTOR, which favors the 5-indole isomer,[15d] ATR has a clear preference for the 4-substituted indole compared with either of the 5- or 6-indole isomers. We also synthesized the 7-indole analogue **9**, which we found to be of intermediary potency presumably by virtue of being able to adopt a similar conformation and have shape complementarity

Table 1. PIKK-Family Enzyme and Cell Inhibitory Potency for Screening Hit 5

ATR IC_{50} (μM)[a]	ATR LE[b]	mTOR IC_{50} (μM)[a,c]	DNA-PK IC_{50} (μM)[a]	PI3Kα IC_{50} (μM)[a,c]	ATR cell IC_{50} (μM)[a,d]	mTOR cell IC_{50} (μM)[a,e]
0.030	0.29	0.33	2.7	3.8	1.1	5.9

[a]Standard error of the mean (SEM) pIC_{50} measurement is ≤0.13 from at least two repeat measurements per test. [b]Ligand efficiency (LE): ATR enzyme pIC_{50}/heavy (non-hydrogen) atom count. [c]IC_{50} derived following acoustic dispensing of compound **5** using a Labcyte Echo 550. [d]Inhibition of pChk1 Ser-345 in HT29 cells exposed to 3 μM 4NQO in the presence of compound **5** for 1 h. [e]Inhibition of pAKT Ser-473 in MDA-MB-468 cells.

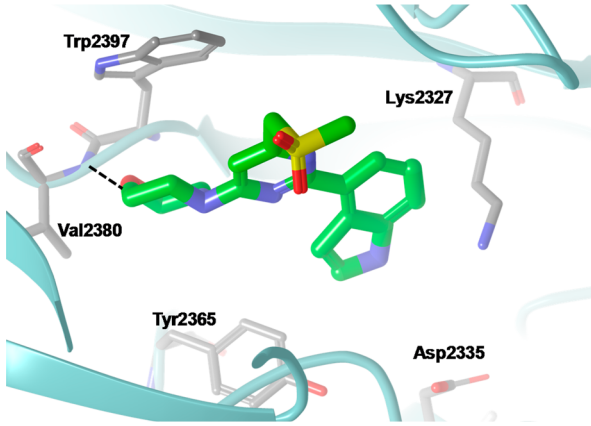

Figure 2. ATR homology model built from an in-house PI3Kγ structure. The binding mode of compound **5** was modeled starting from the morpholinopyrimidine placement observed for compound **2** (PDB structure 3DBS, PI3Kγ).

dx.doi.org/10.1021/jm301859s | *J. Med. Chem.* 2013, 56, 2125−2138

Table 2. Structures and ATR Inhibitory Potency of Compounds 7−10 Compared with 5

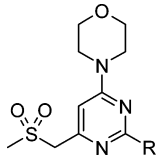

Compound	R	ATR IC_{50} (μM)[a]	ATR cell IC_{50} (μM)[b]	LE
5		0.030	1.1	0.29
7		1.7	>30	0.22
8		1.5	>30	0.22
9		0.18	>30	0.26
10	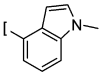	3.3	>30	0.20

[a]Uncertainty (95% confidence) for pIC_{50} measurements is 0.38 (2.4-fold) based on an average of two repeat measurements per compound; compound 7, N = 1. [b]Uncertainty (95% confidence) for pIC_{50} measurement is 0.45 (2.8-fold) based on an average of two repeat occasions per compound.

Table 3. Structures and ATR Inhibitory Potency of Compounds 11−15 Compared with 5

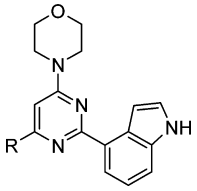

Compound	R	ATR IC_{50} (μM)[a]	ATR cell IC_{50} (μM)[b]	LE	$LogD_{7.4}$[c]	LLE[d]
5		0.030	1.1	0.29	1.7	4.3
11		0.003	0.28	0.30	2.7	3.9
12		0.008	0.36	0.29	2.2	4.3
13		0.004	0.18	0.27	2.4	4.3
14	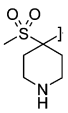	0.009	0.42	0.26	0.7	5.7
15	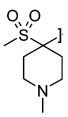	0.061	3.7	0.23	1.9	3.5

[a]Uncertainty (95% confidence) for pIC_{50} measurements is 0.38 (2.4-fold) based on an average of two repeat occasions per compound. [b]Uncertainty (95% confidence) for pIC_{50} measurement is 0.45 (2.8-fold) based on an average of two repeat occasions per compound. [c]Measured using shake-flask methodology with a buffer/octanol volume ratio of 100:1. The concentration of compound in the aqueous phase before and after partitioning with octanol was determined by generic HPLC−UV analysis. [d]Lipophilicity ligand efficiency (LLE): ATR cell pIC_{50} − log $D_{7.4}$.

with **5** but able only to present a C−H group in place of an N−H hydrogen-bond donor contact. N-Methylation of the indole N−H in **5** further confirmed the importance of this group and resulted in near-ablation of ATR potency (compound **10**).

Alkylation of the methylene unit in the sulfone side chain led to an increase in ATR potency (Table 3). Acyclic groups such as the *gem*-dimethyl **11** and three- to six-membered rings (e.g., cyclopropyl **12**, tetrahydropyran **13**, and piperidine **14**) were constructed, and in each case the increase in ATR enzyme potency was found to mirror an increase in cellular potency. The *gem*-dimethyl, cyclopropyl, and tetrahydropyran linkers increase potency with a simultaneous increase in lipophilicity compared with **5**. We favor ligand efficiency (LE), calculated as enzyme pIC_{50}/number of heavy (non-hydrogen) atoms, and ligand lipophilicity efficiency (LLE), calculated as cellular pIC_{50} − log $D_{7.4}$, indices to guide quality in lead discovery and optimization.[23−26] Both indices have the advantage of being simple to calculate, but of greater significance is LLE being a balance of two of the most fundamental parameters to drug designers, namely, cellular potency and lipophilicity. Compounds **11**−**14** maintain high LE; however, the *gem*-dimethyl linker in **11** results in a decreased LLE compared to **5** (3.9 vs 4.3), whereas its cyclopropyl and tetrahydropyran counterparts **12** and **13** have LLE values identical to that of **5**. The charged piperidine **14** (pK_a = 8.8) leads to a significant reduction in log $D_{7.4}$ at the same time as retaining potency in the ATR enzyme and cell assay, thus leading to a significant increase in LLE compared to **5** (5.7 vs 4.3). Compounds **11**−**14** have excellent selectivity over PI3K but retain activity against mTOR (Table 4). These compounds have low micromolar activity in the mTOR cell assay, comparing favorably with <1 μM ATR-driven cellular potency. The moderate lipophilicity of the neutral alkylated sulfonylmorpholinopyrimidine series leads to high free drug in rat plasma, and the compounds show low inhibition of the hERG ion channel. As such, these compounds were deemed of sufficient quality to explore their properties in vivo.

Compounds **11**, **12**, and **13** have low crystalline aqueous solubility, with the solubility of **11** being unmeasurable at pH7.4, but high permeability in Caco-2 cells and reasonable stability to rat hepatocytes in vitro. In contrast, the charged piperidine group in **14** leads to much higher aqueous solubility and unbound fraction all without negatively impacting hERG potency. However, the high basicity of the unsubstituted piperidine group in **14** was a concern for permeability; therefore, we explored substitution on the nitrogen atom. One such compound made, the N-methylated derivative **15**, is shown in Table 3. Unfortunately compound **15** together with several other groups we explored resulted in a reduction in potency compared with the unsubstituted piperidine **14**. Compounds **11**−**14** were formulated as solutions in propylene glycol, to minimize effects of solubility, and dosed orally in Han−Wistar rats. Despite its low aqueous solubility, compound **12** leads to a high AUC (Table 4); however, significantly lower

dx.doi.org/10.1021/jm301859s | J. Med. Chem. 2013, 56, 2125−2138

Table 4. Selectivity and Property Data for Compounds 11−14

compound	mTOR IC_{50} (μM)[a]	PI3Kα IC_{50} (μM)[a]	mTOR cell IC_{50} (μM)[a]	% free (rat)[b]	hERG IC_{50} (μM)[c]	solubility, pH 7.4 (μM)[d]	Caco-2 A−B (pH 6.5)[e]	rat Cl_{int}[f]	rat AUC (μM·h)[g]
11	0.19	1.6	2.7	20	>33	<0.4	16	41	0.76
12	0.18	0.94	3.2	23	>100	4.4	21	<3	3.1
13	nd	1.4	3.3	25	>33	1.8	28	23	0.32
14	0.23	2.7	1.5	40	>33	230[h]	0.2	9.4	0.04

[a]Standard error of the mean (SEM) pIC_{50} measurement is ≤0.42 from at least two repeat measurements per test. nd = not determined. [b]Run in 10% plasma; % free calculated for 100% plasma assuming a single-site binding model. [c]Activity against the human ether-a-go-go-related gene (hERG) encoded potassium channel was determined using automated whole-cell electrophysiology.[28] [d]Solid material agitated in 0.1 M pH 7.4 phosphate buffer for 24 h, double centrifuged, and the supernatant analyzed for compound concentration by LC−UV−MS. Crystallinity assessed by polarized light microscopy of remaining solid. [e]Median A to B P_{app} (1×10^{-6} cm/s), 10 μM compound concentration. [f]Median Cl_{int}: intrinsic clearance from rat hepatocytes (μL/min per 1×10^6 cells, 1 μM compound concentration). [g]Compounds were dosed orally to male Han−Wistar rats at 4 μmol/kg formulated in propylene glycol. [h]Semicrystalline sample.

AUCs were observed with the other linker groups. In particular the poorer in vitro permeability for piperidine **14** is borne out with the lowest exposure seen of all the compounds examined. In a rat PK study, compound **12** has a moderate volume of distribution (2.1 L/kg), moderate plasma clearance (15 mL min^{-1} kg^{-1}) and excellent bioavailability (70%). A much higher exposure, and therefore higher dose, of **12** was required in order to probe ATR inhibition in vivo because of moderate cellular potency. When the dose of compound **12** was increased to 200 mg/kg, formulated as a suspension, increased exposure was accompanied by increased variability. Therefore, compound **12** was not considered a suitable probe molecule for further studies to investigate ATR pharmacology in vivo.

The reasonable LLE, selectivity for ATR over other PIKK-family kinases, and promising PK profile of the cyclopropylsulfone **12**, despite low solubility, made this compound an ideal start point for an early lead optimization campaign. In the next phase we fixed the cyclopropylsulfone linker and explored optimization of the rest of the molecule with a goal to improve solubility and cellular potency while maintaining high permeability and low clearance. A crystalline sample of **12** showed a sharp melt at 221 °C indicative of efficient crystal packing, thus leading to low solubility despite moderate lipophilicity. A single-crystal X-ray structure of **12** was obtained in order to understand crystal packing (Figure 3, CCDC 916869). Compound **12** occupies a P-1 space group, and its solid-state structure shows a centrosymmetric methylsulfone to methylsulfone contact as well as ring−ring stacking and hydrogen bonds between indole N−H and sulfone oxygen in the crystal lattice. From an analysis of small-molecule structures in the Cambridge Structural Database (CSD),[27] we conclude that such methylsulfone contacts are a preferred motif in crystals of methylsulfone compounds, and the motif seems to be associated with low solubility and high melting points. We were intent on retaining the sulfone moiety in order to maintain potency and selectivity. However, making a significant impact on solubility was thought likely to be a challenge given the efficient crystal packing shown in Figure 3. In order to improve solubility, we were left options including disrupting crystal packing, reducing lipophilicity significantly, or introducing charged groups without negatively impacting potency or permeability.

A selection of the compounds made to explore substitution of the terminal methyl group of the sulfone is shown in Table 5 (compounds **16**−**20**). The methylsulfone in **12** can be substituted for larger groups but with a loss of LE. Higher alkyls such as isopropyl (compound **16**), saturated cyclo-heteroalkyls (compounds **17** and **18**), and aromatic groups

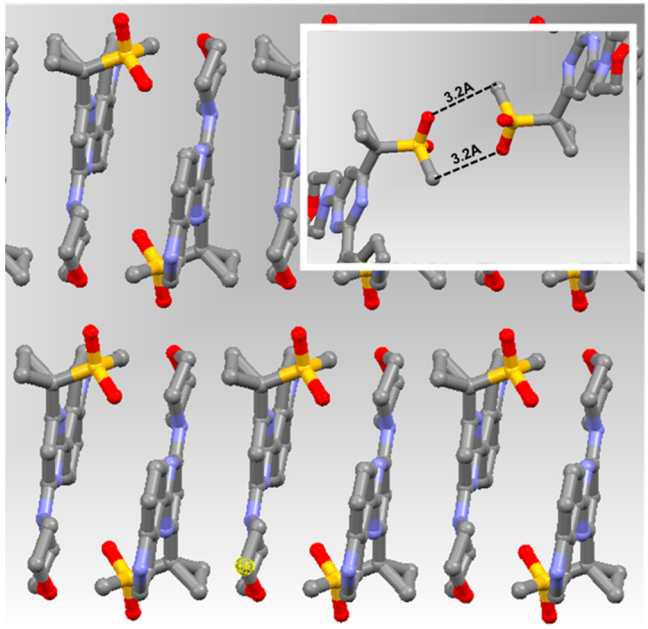

Figure 3. Single crystal X-ray structure of compound **12** (CCDC 916869). Inset picture: methylsulfone−methylsulfone contact.

(compounds **19** and **20**) all retained potency but with decreased LE relative to **12**. Neutral groups that had similar or lower lipophilicity did not improve solubility. Where a charged group was employed, high solubility could be achieved, but in all cases in this position of the molecule, cellular potency was disappointing. We concluded that while this part of the molecule tolerated a broad range of structural variation and offered a way to introduce polar functionality, it was again an unproductive compromise because effects on properties came at the expense of LE; a simple methylsulfone seemed optimal to balance potency and properties.

The SAR of the pyrimidinyl 2-substituent was similarly uncompromising. Replacing the 4-indole with a phenyl group (Table 5, compound **21**) resulted in a loss of >30-fold of potency. We attempted to reintroduce an N−H hydrogen bond in a fashion similar to that achieved with the indole, bearing in mind the limited ways of achieving this without adversely affecting conformation, balance of N−H hydrogen bond strength, lipophilic environment, and shape complementarity. Addition of an amino group to the phenyl ring in **21** to give compound **22** resulted in a reduction in potency. In the mTOR series the indole could be effectively replaced with 4-phenylamides and ureas.[15d] For ATR, however, we thought it

dx.doi.org/10.1021/jm301859s | J. Med. Chem. 2013, 56, 2125−2138

Table 5. Structures and ATR Inhibitory Potency of Compounds 16−25

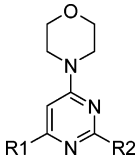

Compound	R1	R2	ATR IC_{50} (μM)[a]	ATR cell IC_{50} (μM)[b]	LE
16			0.013	0.77	0.26
17	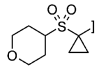		0.033	2.8	0.23
18	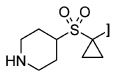		0.046	2.9	0.22
19	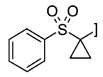		0.005	0.59	0.25
20			0.033	2.0	0.23
21			0.36	>30	0.26
22			1.2	>30	0.23
23			0.12	16	0.24
24			0.13	13	0.25
25			0.18	8.9	0.24

[a]Uncertainty (95% confidence) for pIC_{50} measurements is 0.38 (2.4-fold) based on an average of two repeat occasions per compound. [b]Uncertainty (95% confidence) for pIC_{50} measurement is 0.45 (2.8-fold) based on an average of two repeat occasions per compound; compound **25**, $N = 1$.

unlikely that simple amide and urea derivatives of the aminophenyl **22** would lead to potent inhibitors because it is unlikely that the preferred conformation of such groups would place the N−H bond in a vector similar to that of the 4-indole N−H. However, cyclic amides such as the indolone **23** theoretically are able to place an N−H bond in a similar position. Disappointingly, compound **23** showed only weak ATR enzyme potency, potentially a result of a clash of the indolone oxygen with the protein and/or resulting in a nonplanar torsion relative to pyrimidine and thus leading to less optimal positioning in the binding site. We anticipated being able to replace the indole with other 6,5-heteroaryl groups, in particular with an indazole group as found in the PI3K inhibitor **2**. Much to our disappointment, the indazole **24** was significantly less active than the corresponding indole despite being able to present a similarly strong N−H hydrogen bond to the protein backbone. Perhaps less surprising was the result with benzimidazole **25**, which results in a similarly large reduction in ATR potency. The most likely conformation of this compound is to present an acceptor in place of the indole N−H while the tautomeric N−H forms an internal hydrogen bond with the pyrimidine nitrogen. We concluded that the 4-indole group in compound **12** is a preferred moiety that balances torsional preference and fits into ATR. With this in mind we next set about to examine the opportunity to add additional groups onto the indole ring. A "methyl scan" of compound **12** (Table 6, compounds **26**−**30**) indicated that

Table 6. Structures and ATR Inhibitory Potency of Compounds 26−39

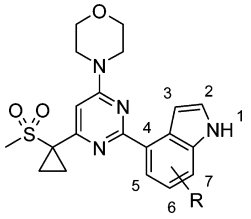

compound	R	ATR IC_{50} (μM)[a]	ATR cell IC_{50} (μM)[b]	LE
26	2-Me	0.028	2.5	0.26
27	3-Me	14	>30	0.17
28	5-Me	nd	>30	
29	6-Me	0.008	0.49	0.28
30	7-Me	0.22	6.3	0.23
31	2-$CONH_2$	1.1	>30	0.19
32	2-CN	0.30	7.2	0.22
33	6-CN	0.066	1.5	0.24
34	6-$CONMe_2$	0.72	24	0.19
35	6-CONHMe	0.14	15	0.21
36	6-$CONH_2$	0.041	9.2	0.24
37	6-F	0.015	0.44	0.27
38	6-Cl	0.016	0.72	0.27
39	6-OMe	0.023	0.80	0.25

[a]Uncertainty (95% confidence) for pIC_{50} measurements is 0.38 (2.4-fold) based on an average of two repeat occasions per compound. nd = not determined. [b]Uncertainty (95% confidence) for pIC_{50} measurement is 0.45 (2.8-fold) based on an average of two repeat occasions per compound; compound **29**, $N = 1$.

positions 2 and, in particular, 6 of the indole were capable of tolerating substituents with the 3- and 5-Me analogues (compounds **27** and **28**), causing a large reduction in potency. The results for the latter substituents are most likely driven by increasing the torsion between indole and pyrimidine rings. Increasing this torsion, however, led to an increase in crystalline solubility (e.g., for compound **28**, pH 7.4, aqueous solubility of 96 μM) and reiterated the difficulty of reducing packing interactions in order to improve solubility while in tandem maintaining potency. A wider set of substituents in positions 2 and 6 of the indole ring were investigated (Table 6, compounds **31**−**39**). The compounds made were a result of the desire to explore a wide enough range of groups in order to affect lipophilicity and make additional binding interactions or affect those interactions in place already, in combination with synthetic expedience. Compounds were made from either commercially available indole boronic acids or a direct precursor to them such as the appropriate 4-bromoindoles. While facile availability of such building blocks is limited, sufficient diversity was available to explore the majority of

dx.doi.org/10.1021/jm301859s | J. Med. Chem. 2013, 56, 2125−2138

substituents of interest. Substituents in the 2-position, such as the carboxamido and cyano groups (compounds **31** and **32**), led to a large reduction in ATR potency compared with methyl. As indicated by the methyl scan, a broader range of substituents were indeed tolerated in the 6-position (compounds **33**−**39**). However, only simple substituents such as 6-F (compound **37**), 6-Cl (compound **38**), and 6-OMe (compound **39**) resulted in broad retention of LE and cellular potency and none of these groups were predicted nor found to improve solubility. Although an exhaustive set of substituents has not been described, our goal of substantially moving potency and physical properties had not been realized although certain substituents on the indole ring, such as fluoro, might have additional utility such as blocking specific sites of metabolism.

We next turned our attention to the morpholine group in compound **12**. Interestingly the 3(*S*)-methylmorpholine **40** (Table 7) led to a tandem reduction of ATR enzyme and cellular potency despite being a preferred group for affinity in mTOR.[15d] We also made the corresponding 3(*R*)-methylmorpholine, compound **6**, and to our surprise we discovered a clear improvement in ATR enzyme and cell potency compared to morpholine. An analysis involving 15 exact matched pairs revealed an average increase in ATR cell potency of ∼5-fold when morpholine is replaced with a 3(*R*)-methylmorpholine group (Figure 4). The effect on potency is even more striking when the two stereoisomers are compared directly; the *R*-isomer **6** is nearly 100-fold more potent in cells than the corresponding *S*-isomer **40**. Moreover the 3(*R*)-methyl group produces interesting effects on selectivity in addition to modest improvements of physical properties. We discovered that while potency against recombinant mTOR enzyme increases compared with **12**, compound **6** has improved PI3K selectivity and notably the difference between ATR cellular and the mTOR (pAKT) cell potency clearly increases in **6** compared with **12** (Figure 5). Similar PI3K selectivity results for compounds containing the 3(*R*)-methylmorpholine hinge binder were subsequently described by Zask et al. for a series of mTOR inhibitors.[15b] A crystal structure of compound **6** (not shown, CCDC 915814) shows similar methylsulfone stacking, but **6** displays a different symmetry in the solid state from that seen with **12**. The morpholine 3(*R*)-methyl prefers to occupy an axial position, as the aromatic linked nitrogen adopts an sp^2 geometry, thus forcing the methyl to be axial. On the basis of this structure, we hoped for an improvement in solubility. The crystalline melting point of compound **6**, albeit still relatively high, is reduced to an extent compared with compound **12** (204 °C vs 221 °C) which translated into a small but consistent increase in aqueous solubility (compound **6**, pH 7.4, aqueous solubility of 10 μM). We also explored larger substituents on the morpholine. When the methyl group was replaced with an ethyl group with the same configuration (compound **41**), a significant reduction in potency was observed. Finally, the bridged morpholine, compound **42**, was prepared and found to be equipotent to morpholine albeit with reduced LLE.

Compound **6** seemed to represent a step forward in terms of a probe compound compared with **12**. Compound **6** has improved LLE and excellent free drug levels and does not significantly inhibit the hERG ion channel when measured in a whole cell assay (Table 8).[28] Compound **6** was assessed for drug−drug interaction (DDI) potential specifically from inhibition of cytochrome P450 enzymes.[29] Interestingly, compound **6** shows no significant reversible inhibition of any of the five major cytochrome P450 isoforms, but when tested for time-dependent inhibitory (TDI) activity following incubation with human liver microsomes, **6** was found to inhibit the cytochrome 3A4-mediated metabolism of midazolam by 50% at 10 μM.[30] Inhibition of the CYP3A family of enzymes is of particular concern for DDI given that they are the major metabolizing enzymes involved in the human metabolism of many drug molecules. In addition to DDI, covalent modification associated with TDI can result in toxicological consequences especially in the liver. In a recent study of 400 registered drugs, 16 (4%) were found positive for 3A4 TDI while the proportion was much greater (20%) when lead-optimization chemistry was tested.[31] In addition, although TDI is often coupled with reversible inhibition, 35% of the drugs that were tested TDI positive showed no (>10 μM) reversible inhibition, suggesting that TDI testing is important to fully evaluate DDI risk in the selection of candidate drug molecules.[31] A number of mechanisms for TDI have been proposed including formation of a tight-binding inhibitory metabolite complex or by covalent adduct formation to heme or protein.[29,31] Specific structural features have been linked to cytochrome P450 3A4 metabolism and inactivation,[29,31,32] but a full structural understanding of 3A4 TDI is not available. In the case of compound **6** the precise structural feature(s) responsible for the observed 3A4 TDI remains unknown. In-silico classification models of cytochrome P450 3A4-mediated TDI have been described and are likely to become of increasing importance combined with in vitro screening approaches to allow drug designers to efficiently identify compounds devoid of this activity.[32] Compound **6** has high permeability combined with good stability to rat hepatocytes and, despite the lack of progress in achieving markedly higher solubility, has respectable bioavailability in a low dose rat PK study. Moreover, plasma exposure at moderate oral doses in the mouse was high, relative to in vitro ATR cellular potency, without undue variability. The unbound concentration achieved at 50 mg/kg is below the

Table 7. Structures and ATR Inhibitory Potency of Compounds 40, 6, 41, and 42

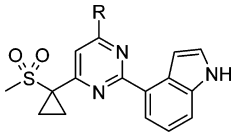

Compound	R	ATR IC_{50} (μM)[a]	ATR Cell IC_{50} (μM)[b]	LE	$LogD_{7.4}$	LLE
40		0.034	3.7	0.26	2.8	2.6
6		0.005	0.050	0.29	2.7	4.6
41		0.17	4.4	0.23	3.0	2.4
42	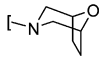	0.007	0.35	0.27	2.6	3.9

[a]Uncertainty (95% confidence) for pIC_{50} measurements is 0.38 (2.4-fold) based on an average of two repeat occasions per compound. [b]Uncertainty (95% confidence) for pIC_{50} measurement is 0.45 (2.8-fold) based on an average of two repeat occasions per compound; compound **41**, $N = 1$.

dx.doi.org/10.1021/jm301859s | J. Med. Chem. 2013, 56, 2125−2138

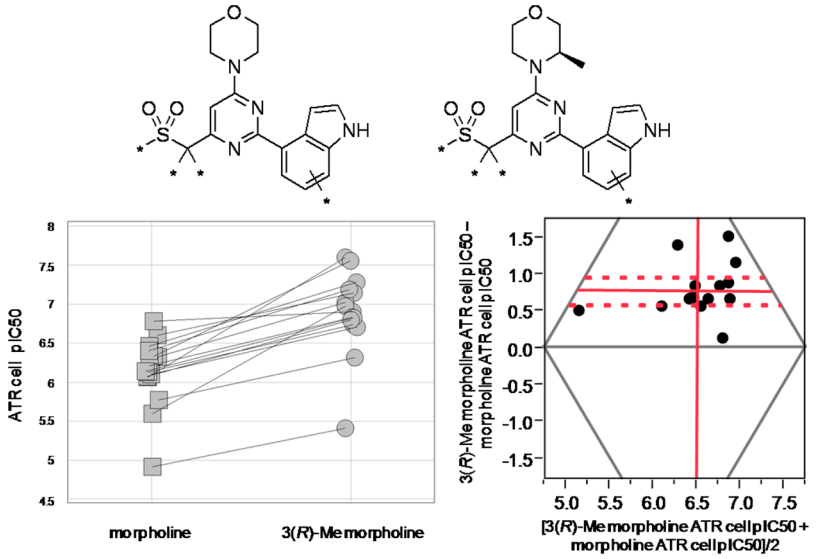

Figure 4. ATR cell potency compared for matched-pair analogues of morpholine and 3(*R*)-Me morpholine hinge binders. Lower left: Each marker represents an individual compound matching the substructure shown. Lines connect exact structural matches (∗ = position of variation). Lower right: Each marker represents a matched pair; mean pIC_{50} difference = 0.765 (SE = 0.09, *N* = 15).

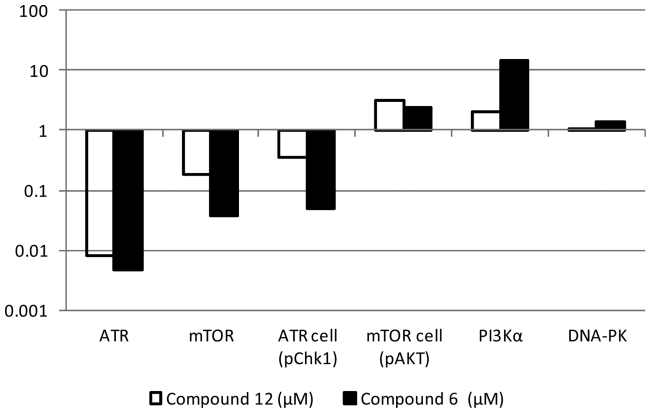

Figure 5. PIKK selectivity compared for compounds **12** and **6**.

mTOR cell (pAKT) IC_{50} while achieving >12 h of exposure over the ATR cell IC_{50} (Figure 6).

Compound **6** is a potent and selective inhibitor of ATR (Table 9). Likewise, with the earlier compounds described in this series, compound **6** inhibits recombinant mTOR enzyme activity, but this leads to only weak potency in the mTOR (pAKT) cell assay. Compound **6** shows good selectivity against all of the PI3K isoforms together with ATM and DNA-PK, and when tested in a large panel of kinases, **6** shows very high general kinase selectivity. Out of a panel of 442 kinases only two, mTOR and PI3Kα, had <50% residual activity when incubated with **6** at 1 μM, representing just 0.5% of the panel tested.[33] Compound **6** leads to potent in vitro inhibition of cell growth in cell lines with high baseline levels of replication stress such as LoVo colorectal adenocarcinoma cells.[34] The combination of potent growth inhibitory effects in vitro and high exposure led to significant antitumor effects in vivo. Female nude mice bearing LoVo tumors were treated with compound **6** orally at a dose of 25 mg/kg twice daily or 50 mg/kg once daily for 13 days. Both schedules led to significant tumor growth inhibition at the end of study compared with vehicle treated controls (Figure 7). Body weight loss was in an acceptable range throughout the study, and compound **6** was generally well tolerated. Compound **6** is the first reported inhibitor of ATR protein kinase demonstrating tumor growth inhibition in vivo and is therefore a useful probe molecule to aid further investigation of ATR tumor biology.

CONCLUSION

Compound **6** was discovered from a lead discovery and early optimization campaign from an mTOR inhibitor screening hit. The sulfonylmorpholinopyrimidine series has good potency and selectivity for ATR, attractive LE and LLE, but low aqueous solubility. Optimization within the confines of the described SAR led to **6**. Compound **6** has 20-fold improved cellular potency compared to the screening hit **5**, retains some residual recombinant mTOR enzyme inhibitory potency, but shows otherwise excellent kinase selectivity. Compound **6** is a poorly soluble compound and is a time-dependent inhibitor of cytochrome 3A4. However, **6** has high mouse free drug exposure at moderate doses despite its low solubility and shows tumor growth inhibition in LoVo xenografts in vivo at well

Table 8. Property and PK Data for Compound 6

% free (rat)	hERG IC_{50} (μM)	3A4 IC_{50} (μM)[a]	3A4 TDI % inhibition, 10 μM[b]	solubility, pH 7.4 (μM)	Caco-2 A−B (pH 6.5) (1×10^{-6} cm/s)	rat Cl_{int}	rat bioavailability (%)[c]
15	50	>10	50	10	23	9.5	62

[a]>10 μM vs 1A2, 2C19, 2C9, and 2D6. [b]Mean value (*N* = 4). Compound **6** was preincubated at 10 μM with human liver microsomes (1 mg/mL) with and without NADPH (5 mM) for 30 min at 37 °C followed by 15 min of incubation with 10 μM midazolam. Analysis of 1-hydroxymidazolam was performed using liquid chromatography−tandem mass spectrometry.[30] No activity was detected vs control for 1A2, 2C19, 2C9, and 2D6. [c]Compound **6** was administered orally to male Han−Wistar rats at 4 μmol/kg formulated as a solution in propylene glycol.

dx.doi.org/10.1021/jm301859s | J. Med. Chem. 2013, 56, 2125−2138

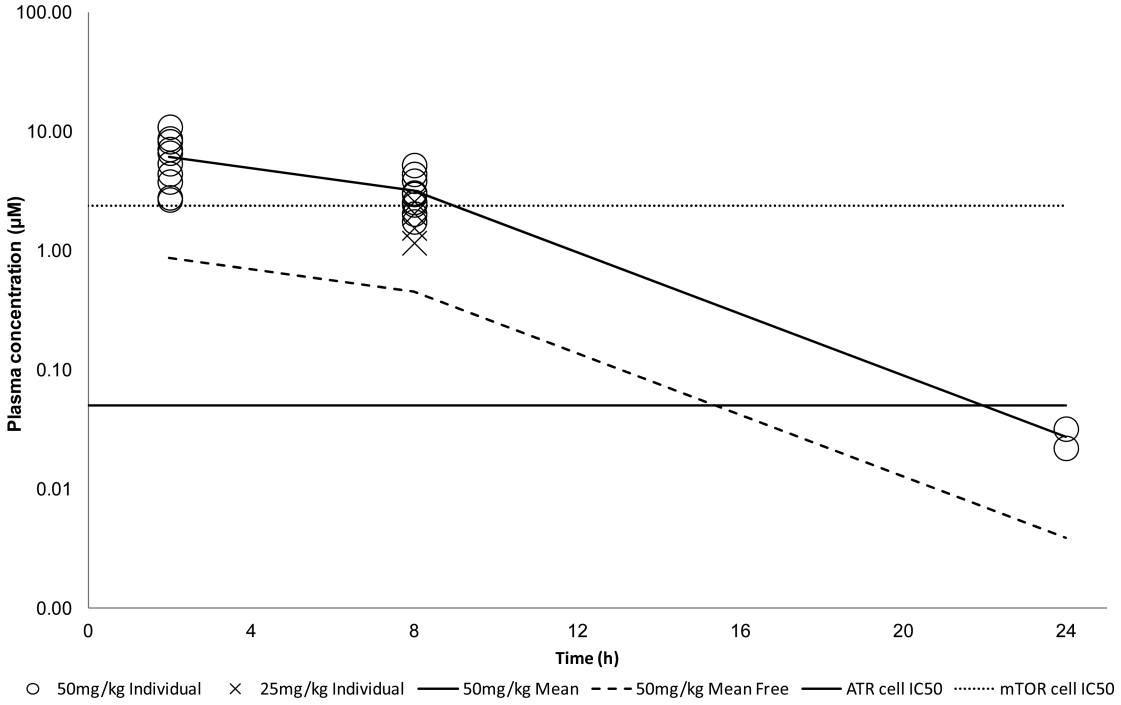

Figure 6. Plasma concentration data in female nude mice dosed with **6** as a solution in 10% DMSO/40% propylene glycol/50% water orally at 25 (×) and 50 mg/kg (○). Data shown are from individual animals. For 50 mg/kg: 2 h, $N = 10$; 8 h, $N = 9$; 24 h, $N = 2$. For 25 mg/kg: 8 h, $N = 4$. Solid line is drawn through mean 50 mg/kg values. Hashed line is unbound concentration. Lower solid line is ATR cell IC_{50} (μM). Upper dotted line is mTOR cell IC_{50} (μM).

Table 9. ATR, PIKK Selectivity, and Growth Inhibitory Potency for Compound 6

ATR IC_{50} (μM)	ATR cell IC_{50} (μM)	mTOR IC_{50} (μM)[a]	mTOR cell IC_{50} (μM)[a]	PI3Kα IC_{50} (μM)[a]	PI3Kα cell IC_{50} (μM)[b]	ATM cell IC_{50} (μM)[c]	DNA-PK cell IC_{50} (μM)[d]	selectivity score $S(50)$[e]	LoVo GI_{50} (μM)[a,f]
0.005	0.050	0.038	2.4	13	>30	>30	>30	0.005	0.20

[a]Standard error of mean (SEM) pIC_{50} measurement is ≤0.22 from at least two repeat measurements per test. [b]Inhibition of pAKT T308 in BT-474 cells. [c]Inhibition of pATM Ser-1981 in HT29 cells. [d]Inhibition of pDNA-PK Ser-2056 in HT29 cells. [e]The fraction of 442 kinases having <50% residual activity in the presence of 1 μM compound **6**. [f]MTS assay with 72 h of continuous exposure to compound **6**.

tolerated doses. Compound **6** is the first reported ATR inhibitor with the required potency, selectivity, and properties to explore ATR pharmacology in vivo.

MATERIALS AND METHODS

General Methods. All experiments were carried out under an inert atmosphere and at room temperature unless otherwise stated. Microwave reactions were performed using one of the following reactors: Biotage initiator, Personal Chemistry Emrys optimizer, Personal Chemistry Smithcreator, or CEM Explorer. Workup procedures were carried out using traditional phase separating techniques or by using strong cation exchange (SCX) chromatography using Isolute SPE flash SCX-2 column (International Sorbent Technology Limited, Mid Glamorgan, U.K.). When necessary, organic solutions were dried over anhydrous $MgSO_4$ or Na_2SO_4. Flash column chromatography (FCC) was performed on Merck Kieselgel silica (article 9385) or on Silicycle cartridges (40–63 μm silica, 4–330 g weight) or on GraceResolv cartridges (4–120 g) either manually or automated using an Isco Combi Flash Companion system. Preparative reverse phase HPLC (RP HPLC) was performed on C18 reversed-phase silica, for example, on a Waters "Xterra" or "XBridge" preparative reversed-phase column (5 μm silica, 19 mm diameter, 100 mm length) or on a Phenomenex "Gemini" or "AXIA" preparative reversed-phase column (5 μm silica, 110A, 21.1 mm diameter, 100 mm length) using decreasingly polar mixtures as eluent, for example, containing 1–5% formic acid or 1–5% aqueous ammonium hydroxide (d = 0.88) as solvent A and acetonitrile as solvent B or MeOH/MeCN, 3:1. Intermediates were not necessarily fully purified, but their structures and purity were assessed by TLC, NMR, HPLC, and mass spectral techniques and are consistent with the proposed structures. The purities of compounds for biological testing were assessed by NMR, HPLC, and mass spectral techniques and are consistent with the proposed structures; purity was ≥95% except for compound **17** (90%), compound **28** (90%), compound **30** (85%), compound **33** (92%), and compound **37** (89%). Electrospray mass spectral data were obtained using a Waters ZMD or Waters ZQ LC/mass spectrometer acquiring both positive and negative ion data, and generally, only ions relating to the parent structure are reported. Unless otherwise stated, ^{1}H NMR spectra were obtained using a Bruker DRX400 operating at 400 MHz in DMSO-d_6 or $CDCl_3$. Chemical shifts are reported as δ values (ppm) downfield from internal TMS in appropriate organic solutions. Peak multiplicities are expressed as follows: s, singlet; d, doublet; dd, doublet of doublet; t, triplet; br s, broad singlet; m, multiplet. Analytical HPLC was performed on C18 reverse-phase silica, on a Phenomenex "Gemini" preparative reversed-phase column (5 μm silica, 110A, 2 mm diameter, 50 mm length) using decreasingly polar mixtures as eluent, for example, decreasingly polar mixtures of water (containing 0.1% formic acid or 0.1% ammonia) as solvent A and acetonitrile as solvent B or MeOH/MeCN, 3:1, with a flow rate of about 1 mL/min, and detection was by electrospray mass spectrometry and by UV absorbance at a wavelength of 254 nm. Accurate mass spectra were recorded on a Themo LTQ-FT in +ve ion mode with a Thermo Accela pump and Surveyor PDA+ with a CTC autosampler, and the results agreed with the theoretical values to within 4 ppm. Combustion analyses (C, H, N) were performed with a Carlo Erba

dx.doi.org/10.1021/jm301859s | J. Med. Chem. 2013, 56, 2125–2138

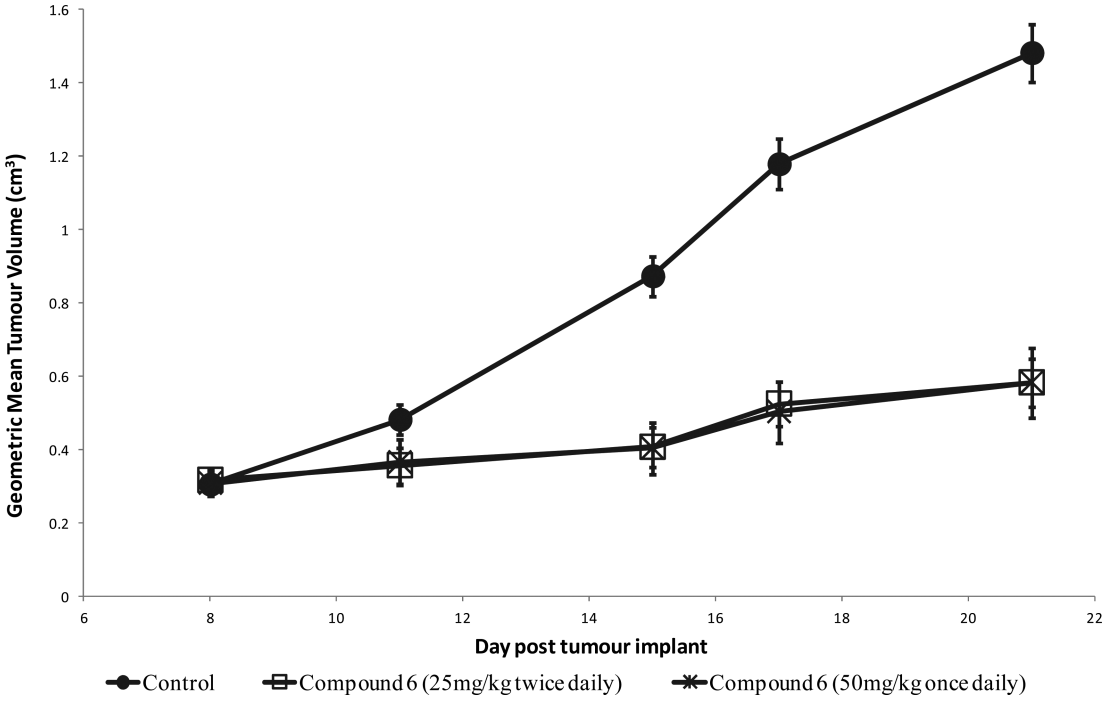

Figure 7. In vivo tumor growth inhibition (TGI) for compound **6**. Female nude mice bearing established human LoVo colorectal adenocarcinoma xenografts were dosed orally with either vehicle (●) or **6** at 25 mg/kg twice daily (□, day 21 TGI = 78%, $p < 0.0005$) and 50 mg/kg once daily (×, day 21 TGI = 77%, $p < 0.0005$) from day 9 to day 21.

EA1108 analyzer, and the results agreed with the theoretical values to within ±0.5%. Water was measured by the Karl Fischer method using a Mettler DL 18.

4-{4-[(3*R*)-3-Methylmorpholin-4-yl]-6-[1-(methylsulfonyl)-cyclopropyl]pyrimidin-2-yl}-1*H*-indole (6). Bis-(triphenylphosphine)palladium chloride (1.692 g, 2.41 mmol), compound **77** (8.00 g, 24.1 mmol), 1*H*-indol-4-ylboronic acid (4.27 g, 26.5 mmol), and 2 M aqueous Na_2CO_3 (36.2 mL, 72.3 mmol) were suspended in 4:1 DME/water (170 mL) and heated to 90 °C overnight. The DME was removed and the reaction mixture diluted with EtOAc (100 mL). The mixture was washed with water (2 × 100 mL). The organics were separated, filtered through a pad of Celite, and concentrated in vacuo onto silica. The residue was purified by chromatography on silica with an elution gradient of 0−10% EtOAc in DCM. Fractions containing product were combined and evaporated. The residue was purified by chromatography on silica, eluting with a gradient of 0−25% EtOAc in DCM. Fractions containing product were combined and evaporated onto reverse phase C18 silica. The crude product was purified by reverse phase using a 415g HP C18 column using decreasingly polar mixtures of water (containing 1% NH_3) and MeCN as eluents. Fractions containing product were combined and evaporated. The residue was taken up in dry MeOH and dried over $MgSO_4$. The mixture was filtered and the solvent evaporated, leaving a gum. The gum was dissolved in DCM (500 mL), filtered and the solvent removed under reduced pressure. The residue was dissolved in MeOH (50 mL) and allowed to stir at room temperature overnight. The resultant precipitate was collected by filtration to afford **6** (5.10 g, 51%). ^{1}H NMR (DMSO-d_6): 1.29 (3H, d), 1.57−1.64 (2H, m), 1.68−1.78 (2H, m), 3.24−3.31 (1H, td), 3.29 (3H, s), 3.51 (1H, td), 3.67 (1H, dd), 3.80 (1H, d), 4.01 (1H, dd), 4.21 (1H, d), 4.61 (1H, m), 6.85 (1H, s), 7.21 (1H, t), 7.32 (1H, t), 7.46 (1H, t), 7.56 (1H, d), 8.06 (1H, dd), 11.25 (1H, s). ^{13}C NMR (DMSO-d_6): 12.2, 13.3, 38.9, 40.3, 46.1, 46.4, 66.0, 70.2, 100.5, 102.8, 113.7, 120.3, 120.5, 126.0, 126.2, 129.4, 137.0, 161.4, 161.9, 164.4. HRMS-ESI *m/z*: 413.163 97 $[MH]^+$ $C_{21}H_{24}N_4O_3S$ requires 413.164 19. Chiral HPLC: (HP1100 system 4, 5 μm Chiralpak AS-H (250 mm × 4.6 mm) column, eluting with isohexane/EtOH/TEA 60/40/0.1) R_f = 8.815, >99%. Anal. Found (% w/w): C, 60.65; H, 5.83; N, 13.4; S, 7.65; H_2O, <0.3. $C_{21}H_{24}N_4O_3S$ requires C, 61.15; H, 5.86; N, 13.58; S, 7.77.

4-{4-[1-(Methylsulfonyl)cyclopropyl]-6-morpholin-4-ylpyrimidin-2-yl}-1*H*-indole (12). Bis(triphenylphosphine)palladium(II) dichloride (82 mg, 0.12 mmol), **71** (371 mg, 1.17 mmol), 2 M aqueous Na_2CO_3 (3.50 mL, 7.00 mmol), and 1*H*-indol-4-ylboronic acid (225 mg, 1.40 mmol) were suspended in 18% DMF in 7:3:2 DME/water/EtOH (8 mL) and sealed into a microwave tube. The mixture was heated to 110 °C for 1 h in a microwave reactor and then allowed to cool to room temperature. The mixture was purified by preparative HPLC using decreasingly polar mixtures of water (containing 1% NH_3) and MeCN as eluents. Fractions containing the desired compound were combined and then evaporated. The residue was purified by preparative HPLC using decreasingly polar mixtures of water (containing 0.1% formic acid) and MeCN as eluents. Fractions containing the desired compound were combined and then evaporated to afford **12** (264 mg, 57%). ^{1}H NMR (DMSO-d_6): 1.60−1.63 (2H, m), 1.71−1.74 (2H, m), 3.10 (3H, s), 3.74−3.78 (8H, m), 6.89 (1H, s), 7.21 (1H, t), 7.31 (1H, d), 7.46 (1H, t), 7.55 (1H, d), 8.04−8.06 (1H, m), 11.25 (1H, s). ^{13}C NMR (DMSO-d_6): 12.2, 40.3, 44.0, 46.1, 65.8, 100.5, 102.9, 113.7, 120.3, 120.5, 126.2, 129.3, 136.9, 161.5, 162.5, 164.4. HRMS-ESI *m/z*: 399.148 16 $[MH]^+$ $C_{20}H_{22}N_4O_3S$ requires 399.148 54.

(*R*)-Methyl 2-Chloro-6-(3-methylmorpholino)pyrimidine-4-carboxylate (45). (*R*)-3-Methylmorpholine (7.18 g, 71.0 mmol) and triethylamine (12.87 mL, 92.31 mmol) were added to **43** (14.70 g, 71.01 mmol) in DCM (100 mL). The resulting mixture was stirred at room temperature for 18 h. Water (100 mL) was added. The layers were separated and extracted with DCM (5 mL). The combined organics were dried over $MgSO_4$, concentrated in vacuo and the residue was triturated with Et_2O to afford **45** (14.77 g, 77%). ^{1}H NMR ($CDCl_3$): 1.33−1.37 (3H, d), 3.31−3.38 (1H, m), 3.52−3.59 (1H, m), 3.68−3.72 (1H, m), 3.79−3.83 (1H, m), 3.98 (3H, s), 4.02−4.05 (1H, m), 4.12 (1H, m), 4.37 (1H, m), 7.16 (1H, s). MS-ESI *m/z* 272.43 $[MH^+]$. The liquors were concentrated onto silica and purified by chromatography on silica, eluting with a gradient of 20−40% EtOAc in isohexane. Fractions containing product were combined and evaporated to afford **45** (1.659 g, 9%). ^{1}H NMR ($CDCl_3$): 1.33−1.37 (3H, d), 3.31−3.38 (1H, m), 3.52−3.59 (1H, m), 3.68−3.72 (1H, m), 3.79−3.83 (1H, m), 3.98 (3H, s), 4.02−4.05 (1H, m), 4.12 (1H, m), 4.37 (1H, m), 7.16 (1H, s). MS-ESI *m/z* 272.43 $[MH^+]$.

dx.doi.org/10.1021/jm301859s | *J. Med. Chem.* 2013, 56, 2125−2138

(*R*)-(2-Chloro-6-(3-methylmorpholino)pyrimidin-4-yl)-methanol (48). Lithium borohydride, 2 M in THF (18 mL, 36 mmol), was added dropwise to **45** (16.28 g, 59.92 mmol) in THF (200 mL) at 0 °C over a period of 20 min under nitrogen. The resulting solution was stirred at 0 °C for 30 min and then allowed to warm to room temperature and stirred for a further 18 h. Water (200 mL) was added and the THF evaporated. The aqueous layer was extracted with EtOAc (2 × 100 mL) and the organic phases were combined, dried over $MgSO_4$, and then evaporated to afford **48** (14.54 g, 100%) which was used in the next step without purification. ^{1}H NMR ($CDCl_3$): 1.32 (3H, d), 2.65 (1H, br s), 3.25−3.32 (1H, m), 3.51−3.57 (1H, m), 3.67−3.70 (1H, m), 3.78 (1H, d), 3.98−4.09 (2H, m), 4.32 (1H, m), 4.59 (2H, s), 6.44 (1H, s). MS-ESI *m*/*z* 244.40 [MH^+].

(*R*)-4-(2-Chloro-6-(iodomethyl)pyrimidin-4-yl)-3-methylmorpholine (51). (a) Methanesulfonyl chloride (4.62 mL, 59.7 mmol) was added dropwise to **48** (14.54 g, 59.67 mmol) and triethylamine (8.32 mL, 59.7 mmol) in DCM (250 mL) at 25 °C over a period of 5 min. The resulting solution was stirred at 25 °C for 90 min. The reaction mixture was quenched with water (100 mL) and extracted with DCM (2 × 100 mL). The organic phases were combined, dried over $MgSO_4$, filtered, and evaporated to afford (*R*)-(2-chloro-6-(3-methylmorpholino)pyrimidin-4-yl)methyl methanesulfonate (20.14 g, 105%) which was used in the next step without further purification. ^{1}H NMR ($CDCl_3$): 1.33 (3H, d), 3.13 (3H, s), 3.27−3.34 (1H, m), 3.51−3.57 (1H, m), 3.66−3.70 (1H, m), 3.79 (1H, d), 3.99−4.03 (2H, m), 4.34 (1H, m), 5.09 (2H, d), 6.52 (1H, s). MS-ESI *m*/*z* 322.39 [MH^+]. (b) Lithium iodide (17.57 g, 131.27 mmol) was added to (*R*)-(2-chloro-6-(3-methylmorpholino)pyrimidin-4-yl)methyl methanesulfonate (19.2 g, 59.67 mmol) in dioxane (300 mL) and heated to 100 °C for 2 h under nitrogen. The reaction mixture was quenched with water (200 mL) and extracted with EtOAc (3 × 200 mL). The organic layers were combined and washed with 2 M sodium bisulfite solution (400 mL), water (400 mL), brine (400 mL), dried over $MgSO_4$, and then evaporated. The residue was triturated with Et_2O to afford **51** (13.89 g, 66%). ^{1}H NMR ($CDCl_3$): 1.32 (3H, d), 3.24−3.32 (1H, m), 3.51−3.58 (1H, m), 3.67−3.71 (1H, m), 3.78 (1H, d), 3.98−4.02 (2H, m), 4.21 (2H, s), 4.29 (1H, m), 6.41 (1H, s). MS-ESI *m*/*z* 354.31 [MH^+]. The mother liquors were concentrated and triturated with Et_2O to afford a further crop of **51** (2.46 g, 12%). ^{1}H NMR ($CDCl_3$): 1.32 (3H, d), 3.24−3.32 (1H, m), 3.51−3.58 (1H, m), 3.67−3.71 (1H, m), 3.78 (1H, d), 3.98−4.02 (2H, m), 4.21 (2H, s), 4.29 (1H, m), 6.41 (1H, s). MS-ESI *m*/*z* 354.31 [MH^+].

2,4-Dichloro-6-(methylsulfonylmethyl)pyrimidine (54). (a) Compound **53** (175 g, 1.09 mol) was dissolved in DMF (2 L), and then sodium methanesulfinate (133.5 g, 1.31 mol) was added. The mixture was heated to 125 °C for 2 h. After cooling to room temperature, the mixture was filtered and the filtrate was concentrated in vacuo. The crude material was washed with water, filtered, then triturated with toluene. The solid was filtered and then triturated with isohexane to provide 6-(methylsulfonylmethyl)-1*H*-pyrimidine-2,4-dione (250 g), which was used without further purification. (b) 6-(Methylsulfonylmethyl)-1*H*-pyrimidine-2,4-dione (132 g, 0.65 mol) was added to $POCl_3$ (1.2 L), and the mixture was heated to reflux for 16 h. The excess $POCl_3$ was removed in vacuo and the residue azeotroped with toluene (2 × 500 mL) and then dissolved in DCM. This solution was poured slowly onto ice (4 L) (CARE: risk of exotherm), and the mixture was stirred for 20 min. The mixture was extracted with DCM (3 × 1 L) (insoluble black material was filtered off and discarded) and EtOAc (2 × 1 L). The organic extracts were combined, dried, and concentrated in vacuo to give compound **54** (51 g) which was used without further purification. ^{1}H NMR (DMSO-d_6): 3.13 (3H, s), 4.79 (2H, s), 7.87 (1H, s). MS-ESI *m*/*z* 239 [MH^+].

(*R*)-4-(2-Chloro-6-(methylsulfonylmethyl)pyrimidin-4-yl)-3-methylmorpholine (56). Sodium methanesulfinate (4.64 g, 45.5 mmol) was added in one portion to **51** (13.4 g, 37.9 mmol) in DMF (100 mL). The resulting mixture was stirred at 25 °C for 2 h. The reaction mixture was diluted with DCM and washed with water (2 × 100 mL), aqueous sodium thiosulfate (50 mL), dried over $MgSO_4$, and concentrated in vacuo. The residue was triturated with MeOH to give a solid which was dried under vacuum to afford **56** (7.3 g, 63%). ^{1}H NMR (DMSO-d_6): 1.21 (3H, d), 3.12 (3H, s), 3.24 (1H, t), 3.42−3.49 (1H, td), 3.58−3.62 (1H, m), 3.74 (1H, d), 3.93−4.40 (3H, m), 4.47 (2H, s), 6.94 (1H, s). MS-ESI *m*/*z* 306.05 [MH^+]. The mother liquors were purified by chromatography on silica with an elution gradient of 40−90% EtOAc in isohexane. Fractions containing product were combined and evaporated to afford a further crop of **56** (2.0 g, 17%). MS-ESI *m*/*z* 306.12 [MH^+].

2-Chloro-4-(methylsulfonylmethyl)-6-morpholin-4-ylpyrimidine (62). Triethylamine (6.78 mL) was added to a cooled (−5 °C) suspension of **54** (10.56 g, 43.8 mmol) in DCM (230 mL). A solution of morpholine (3.85 mL) in DCM (30 mL) was then added dropwise while keeping the temperature below −5 °C. The mixture was then stirred at room temperature for 1 h. The solution was washed with water (300 mL), dried ($MgSO_4$), and concentrated in vacuo. The residue was purified by chromatography on silica, eluting with 1:1 EtOAc/DCM to afford compound **62** (6.81g, 53%). ^{1}H NMR (DMSO-d_6): 3.12 (3H, s), 3.63 (4H, s), 3.68−3.70 (4H, m), 4.45 (2H, s), 6.96 (1H, s). MS-ESI *m*/*z* 292 [MH^+].

4-(2-Chloro-6-(1-(methylsulfonyl)cyclopropyl)pyrimidin-4-yl)morpholine (71). NaOH solution (9.60 mL, 96.0 mmol) was added to a mixture of **62** (2.80 g, 9.60 mmol), 1,2-dibromoethane (1.654 mL, 19.19 mmol), and TBAB (0.619 g, 1.92 mmol) in toluene (120 mL). The resulting solution was then heated to 60 °C for 3 h. The mixture was concentrated in vacuo to provide a residue which was dissolved in EtOAc (200 mL). The solution was washed with water (200 mL) and then saturated brine (100 mL). The solution was then dried ($MgSO_4$) and concentrated in vacuo. The residue was purified by chromatography on silica, eluting with a gradient of 0−2.5% MeOH in DCM to afford **71** (2.88 g, 94%). ^{1}H NMR (DMSO-d_6): 1.49−1.51 (2H, m), 1.62−1.65 (2H, m), 3.19 (3H, s), 3.66−3.69 (8H, m), 6.96 (1H, s). MS-ESI *m*/*z* 318 [MH^+].

(*R*)-4-(2-Chloro-6-(1-(methylsulfonyl)cyclopropyl)pyrimidin-4-yl)-3-methylmorpholine (77). A 50% aqueous solution of NaOH (42 mL) was added to **56** (12.11 g, 39.60 mmol), 1,2-dibromoethane (3.41 mL, 39.6 mmol), and TBAB (1.277 g, 3.96 mmol) in toluene (120 mL). The resulting slurry was stirred at 60 °C for 3 h, and then an additional portion of 1,2-dibromoethane (1 mL) was added and the mixture stirred for a further 1 h. EtOAc (200 mL) was added and the mixture washed with water (100 mL) and brine (100 mL). The reaction mixture was dried over $MgSO_4$ and concentrated in vacuo. The residue was triturated with MeOH to give a solid which was collected by filtration and dried under vacuum to afford **77** (9.65 g, 73%). ^{1}H NMR (DMSO-d_6): 1.21 (3H, d), 1.48−1.54 (2H, m), 1.61−1.67 (2H, m), 3.20 (1H, td), 3.19 (3H, s), 3.44 (1H, td), 3.58 (1H, dd), 3.72 (1H, d), 3.93 (1H, dd), 3.98−4.10 (1H, m), 4.41 (1H, m), 6.93 (1H, s). MS-ESI *m*/*z* 332.44 [MH^+]. The MeOH mother liquors were reduced in vacuo, and the residue was purified by chromatography on silica with an elution gradient of 10−50% EtOAc in DCM. Fractions containing product were combined and evaporated to afford **77** (2.16 g, 16%). ^{1}H NMR (DMSO-d_6): 1.21 (3H, d), 1.49−1.54 (2H, m), 1.59−1.68 (2H, m), 3.19 (3H, s), 3.20 (1H, td), 3.44 (1H, td), 3.58 (1H, dd), 3.71 (1H, d), 3.93 (1H, dd), 4.04 (1H, m), 4.41 (1H, m), 6.93 (1H, s). MS-ESI *m*/*z* 332.44 [MH^+].

Biological Evaluation. IC_{50} values reported are geometric mean values of at least two independent measurements unless otherwise stated.

ATR Kinase Assay. ATR for use in the in vitro enzyme assay was obtained from HeLa nuclear extract (CIL Biotech, Mons, Belgium) by immunoprecipitation with rabbit polyclonal antiserum raised to amino acids 400−480 of ATR (Tibbetts, R. S.; Brumbaugh, K. M.; Williams, J. M.; Sarkaria, J. N.; Cliby, W. A.; Shieh, S. Y.; Taya, Y.; Prives, C.; Abraham, R. T. A role for ATR in the DNA damage-induced phosphorylation of p53. *Genes Dev.* **1999**, *13*, 152−157) contained in the following buffer: 25 mM HEPES (pH 7.4), 2 mM $MgCl_2$, 250 mM NaCl, 0.5 mM EDTA, 0.1 mM Na_3VO_4, 10% v/v glycerol, and 0.01% v/v Tween 20. ATR-antibody complexes were isolated from nuclear extract by incubating with protein A-Sepharose beads (Sigma, no. P3476) for 1 h and then through centrifugation to recover the beads. In the well of a 96-well plate, 10 μL ATR-containing Sepharose beads

were incubated with 1 μg of substrate glutathione *S*-transferase−p53N66 (NH_2-terminal 66 amino acids of p53 fused to glutathione *S*-transferase were expressed in *E. coli*) in ATR assay buffer (50 mM HEPES (pH 7.4), 150 mM NaCl, 6 mM $MgCl_2$, 4 mM $MnCl_2$, 0.1 mM Na_3VO_4, 0.1 mM DTT, and 10% (v/v) glycerol) at 37 °C in the presence or absence of inhibitor. After 10 min with gentle shaking, ATP was added to a final concentration of 3 μM and the reaction continued at 37 °C for an additional 1 h. The reaction was stopped by addition of 100 μL of PBS, and the reaction was transferred to a white opaque glutathione coated 96-well plate (NUNC no. 436033) and incubated overnight at 4 °C. This plate was then washed with PBS/0.05% (v/v) Tween 20, blotted dry, and analyzed by a standard ELISA (enzyme-linked immunosorbent assay) technique with a phosphoserine 15 p53 (16G78) antibody (Cell Signaling Technology, no. 9286). The detection of phosphorylated glutathione *S*-transferase−p53N66 substrate was performed in combination with a goat anti-mouse horseradish peroxidase-conjugated secondary antibody (Pierce, no. 31430). Enhanced chemiluminescence solution (NEN, Boston, MA) was used to produce a signal, and chemiluminescent detection was carried out via a TopCount (Packard, Meriden, CT) plate reader. The resulting calculated % enzyme activity (activity base, IDBS) was then used to determine the IC_{50} values for the compounds (IC_{50} taken as the concentration at which 50% of the enzyme activity is inhibited).

ATR Cell (pChk1) Assay in HT29 Tumor Cells. Compound dose ranges were created by diluting in 100% DMSO and then further into assay medium (EMEM, 10% FCS, 1% glutamine) using a Labcyte Echo acoustic dispensing instrument. Cells were plated in 384-well Costar plates at 9×10^4 cells per mL in 40 μL of EMEM, 10% FCS, 1% glutamine and grown for 24 h. Following addition of compound the cells were incubated for 60 min. A final concentration of 3 μM 4NQO (prepared in 100% DMSO) was then added using the Labcyte Echo, and the cells were incubated for a further 60 min. The cells were fixed by adding 40 μL of 3.7% v/v formaldehyde solution for 20 min. After removal of fix, cells were washed with PBS and permeabilized in 40 μL of PBS containing 0.1% Triton X-100. The cells were then washed, and 15 μL primary antibody solution (pChk1 Ser345) was added. The plates were incubated at 4 °C overnight. The primary antibody was then washed off, and 20 μL of secondary antibody solution (goat anti-rabbit Alexa Fluor 488, Invitrogen) and 1 μM Hoechst 33258 (Invitrogen) added for 90 min at room temperature. The plates were washed and left in 40 μL of PBS. Plates were then read on an ArrayScan VTI instrument to determine staining intensities, and dose responses were obtained and used to determine the IC_{50} values for the compounds.

In Vivo Studies. All animal experiments were conducted in full accordance with the U.K. Home Office Animal (Scientific Procedures) Act 1986. Female Swiss nu/nu mice (AstraZeneca, U.K.) were housed in negative pressure isolators (PFI Systems Ltd., Oxon, U.K.). LoVo tumor xenografts were established in 8- to 12-week-old mice by injecting 1×10^7 tumor cells subcutaneously (100 μL in serum free medium) on the left dorsal flank. Animals were randomized into treatment groups when tumors became palpable. Compound **6** was prepared in 10% DMSO/40% propylene glycol/50% water and administered orally. Tumors were measured up to three times per week with calipers. Tumor volumes were calculated and the data plotted using the geometric mean for each group versus time.

■ ASSOCIATED CONTENT

Supporting Information

Experimental details and data for compounds **7**−**11**, **13**−**42**, **44**, **46**, **47**, **49**, **50**, **52**, **55**, **57**−**61**, **63**−**70**, **72**−**76**, **78**, **80**, **82**−**89**. This material is available free of charge via the Internet at http://pubs.acs.org.

■ AUTHOR INFORMATION

Corresponding Author

*Telephone: +44(0)1625 518629. E-mail: kevin.foote@astrazeneca.com.

Notes

The authors declare no competing financial interest.

■ ACKNOWLEDGMENTS

We acknowledge the excellent technical expertise of the scientists at KuDOS and AstraZeneca, in particular Lisa Smith, Victoria Pearson, Aaron Cranston, and Elaine Brown for biological evaluation, Paul Davey for help with mass spectra analysis, and Drs. Matt Wood, Chris Jones, Robin Smith, Cliff Jones, and Jason Kettle for helpful discussions in preparation of this manuscript.

■ ABBREVIATIONS USED

ATM, ataxia telangiectasia mutated; ATR, ataxia telangiectasia mutated and RAD3-related; DNA-PK, DNA-activated protein kinase; DDR, DNA-damage response; SSB, single strand break; mTOR, mammalian target of rapamycin; PIKK, phosphatidylinositol 3-kinase related kinase; 4NQO, 4-nitroquinoline 1-oxide; LLE, ligand lipophilicity efficiency; hERG, human ether-a-go-go-related gene; Cl_{int}, intrinsic clearance; CSD, Cambridge Structural Database; CCDC, Cambridge Crystallographic Data Centre; TDI, time-dependent inhibition; TGI, tumor growth inhibition; SCX, strong cation exchange; TEA, triethylamine; MeCN, acetonitrile; HATU, *O*-(7-azabenzotriazol-1-yl)-*N*,*N*,*N*′,*N*′-tetramethyluronium hexafluorophosphate

■ REFERENCES

(1) Cimprich, K. A.; Cortez, D. ATR: an essential regulator of genome integrity. *Nat. Rev. Mol. Cell Biol.* **2008**, *9*, 616−627.

(2) Nyberg, K. A.; Michelson, R. J.; Putnam, C. W.; Weinert, T. A. Toward maintaining the genome: DNA damage and replication checkpoints. *Annu. Rev. Genet.* **2002**, *36*, 617−656.

(3) Shechter, D.; Costanzo, V.; Gautier, J. Regulation of DNA replication by ATR: signaling in response to DNA intermediates. *DNA Repair* **2004**, *3*, 901−908.

(4) Wright, J. A.; Keegan, K. S.; Herendeen, D. R.; Bentley, N. J.; Carr, A. M.; Hoekstra, M. F.; Concannon, P. Protein kinase mutants of human ATR increase sensitivity to UV and ionizing radiation and abrogate cell cycle checkpoint control. *Proc. Natl. Acad. Sci. U.S.A.* **1998**, *95*, 7445−7450.

(5) Reduction of ATR activity by siRNA or ATR knock-in using a dominant negative form of ATR in cancer cells results in sensitization to the effects of antimetabolites, alkylating agents, or double-strand break inducers. See the following: (a) Cortez, D.; Guntuku, S.; Qin, J.; Elledge, S. J. ATR and ATRIP: partners in checkpoint signaling. *Science* **2001**, *294*, 1713−1716. (b) Collis, S. J; Swartz, M. J.; Nelson, W. G.; DeWeese, T. L. Enhanced radiation and chemotherapy-mediated cell killing of human cancer cells by small inhibitory RNA silencing of DNA repair factors. *Cancer Res.* **2003**, *63*, 1550−1554. (c) Cliby, W. A.; Roberts, C. J.; Cimprich, K. A.; Stringer, C. M.; Lamb, J. R.; Schreiber, S. L.; Friend, S. H. Overexpression of a kinase-inactive ATR protein causes sensitivity to DNA-damaging agents and defects in cell cycle checkpoints. *EMBO J.* **1998**, *17*, 159−169.

(6) Wilsker, D.; Bunz, F. Loss of ataxia telangiectasia mutated- and Rad3-related function potentiates the effects of chemotherapeutic drugs on cancer cell survival. *Mol. Cancer Ther.* **2007**, *6*, 1406−1413.

(7) Sarkaria, J. N.; Busby, E. C.; Tibbetts, R. S.; Roos, P.; Taya, Y.; Karnitz, L. M.; Abraham, R. T. Inhibition of ATM and ATR kinase activities by the radiosensitizing agent, caffeine. *Cancer Res.* **1999**, *59*, 4375−4382.

(8) Prevo, R.; Fokas, E.; Reaper, P. M.; Charlton, P. A.; Pollard, J. R.; McKenna, W. G.; Muschel, R. J.; Brunner, T. B. The novel ATR inhibitor VE-821 increases sensitivity of pancreatic cancer cells to radiation and chemotherapy. *Cancer Biol. Ther.* **2012**, *13*, 1072−1081.

(9) Charrier, J.-D.; Durrant, S. J.; Golec, J. M. C.; Kay, D. P.; Knegtel, R. M. A.; MacCormick, S.; Mortimore, M.; O'Donnell, M. E.; Pinder,

J. L.; Reaper, P. M.; Rutherford, A. P.; Wang, P. S. H.; Young, S. C.; Pollard, J. R. Discovery of potent and selective inhibitors of ataxia telangiectasia mutated and Rad3 related (ATR) protein kinase as potential anticancer agents. *J. Med. Chem.* **2011**, *54*, 2320−2330.
(10) (a) Kaelin, W. G. The concept of synthetic lethality in the context of anticancer therapy. *Nat. Rev. Cancer* **2005**, *5*, 689−698. (b) Collins, I.; Garrett, M. D. Targeting the cell division cycle in cancer: CDK and cell cycle checkpoint kinase inhibitors. *Curr. Opin. Pharmacol.* **2005**, *5*, 366−373.
(11) Toledo, L. I.; Murga, M.; Fernandez-Capetillo, O. Targeting ATR and Chk1 kinases for cancer treatment: a new model for new (and old) drugs. *Mol. Oncol.* **2011**, *5*, 368−373.
(12) Smith, G. C. M.; Jackson, S. P. *Handbook of Cell Signalling*; Elsevier Academic Press: New York, 2003; Vol. *1*, pp 557−561.
(13) Finlay, M. R. V.; Griffin, R. J. Modulation of DNA repair by pharmacological inhibitors of the PIKK protein kinase family. *Bioorg. Med. Chem. Lett.* **2012**, *22*, 5352−5359.
(14) Walker, E. H.; Pacold, M. E.; Perisic, O.; Stephens, L.; Hawkins, P. T.; Wymann, M. P.; Williams, R . L. Structural determinants of phosphoinositide 3-kinase inhibition by wortmannin, LY294002, quercetin, myricetin, and staurosporine. *Mol. Cell* **2000**, *6*, 909−919.
(15) Reviewed in ref 13. For specific examples see the following: (a) Folkes, A. J.; Ahmadi, K.; Alderton, W. K.; Alix, S.; Baker, S. J.; Box, G.; Chuckowree, I. S.; Clarke, P. A.; Depledge, P.; Eccles, S. A.; Friedman, L. S.; Hayes, A.; Hancox, T. C.; Kugendradas, A.; Lensun, L.; Moore, P.; Olivero, A. G.; Pang, J.; Patel, S.; Pergl-Wilson, G. H.; Raynaud, F. I.; Robson, A.; Saghir, N.; Salphati, L.; Sohal, S.; Ultsch, M. H.; Valenti, M.; Wallweber, H. J. A.; Wan, N. C.; Wiesmann, C.; Workman, P.; Zhyvoloup, A.; Zvelebil, M. J.; Shuttleworth, S. J. The identification of 2-(1*H*-indazol-4-yl)-6-(4-methanesulfonyl-piperazin-1-ylmethyl)-4-morpholin-4-yl-thieno[3,2-*d*]pyrimidine (GDC-0941) as a potent, selective, orally bioavailable inhibitor of class I PI3 kinase for the treatment of cancer. *J. Med. Chem.* **2008**, *51*, 5522−5532. (b) Zask, A.; Kaplan, J.; Verheijen, J. C.; Richard, D. J.; Curran, K.; Brooijmans, N.; Bennett, E. M.; Toral-Barza, L.; Hollander, I.; Ayral-Kaloustian, S.; Yu, K. Morpholine derivatives greatly enhance the selectivity of mammalian target of rapamycin (mTOR) inhibitors. *J. Med. Chem.* **2009**, *52*, 7942−7945. (c) Cohen, F.; Bergeron, P.; Blackwood, E.; Bowman, K. K.; Chen, H.; Dipasquale, A. G.; Epler, J. A.; Koehler, M. F. T.; Lau, K.; Lewis, C.; Liu, L.; Ly, C. Q.; Malek, S.; Nonomiya, J.; Ortwine, D. F.; Pei, Z.; Robarge, K. D.; Sideris, S.; Trinh, L.; Truong, T.; Wu, J.; Zhao, X.; Lyssikatos, J. P. Potent, selective, and orally bioavailable inhibitors of mammalian target of rapamycin (mTOR) kinase based on a quaternary substituted dihydrofuropyrimidine. *J. Med. Chem.* **2011**, *54*, 3426−3435. (d) Finlay, M. R. V.; Buttar, D.; Critchlow, S. E.; Dishington, A. P.; Fillery, S. M.; Fisher, E.; Glossop, S. C.; Graham, M. A.; Johnson, T.; Lamont, G. M.; Mutton, S.; Perkins, P.; Pike, K. G.; Slater, A. M. Sulfonyl-morpholino-pyrimidines: SAR and development of a novel class of selective mTOR kinase inhibitor. *Bioorg. Med. Chem. Lett.* **2012**, *22*, 4163−4168. (e) Hickson, I.; Zhao, Y.; Richardson, C. J.; Green, S. J.; Martin, N. M. B.; Orr, A. I.; Reaper, P. M.; Jackson, S. P.; Curtin, N. J.; Smith, G. C. M. Identification and characterization of a novel and specific inhibitor of the ataxia-telangiectasia mutated kinase ATM. *Cancer Res.* **2004**, *64*, 9152−9159.
(16) Maira, S.-M.; Stauffer, F.; Brueggen, J.; Furet, P.; Schnell, C.; Fritsch, C.; Brachmann, S.; Chene, P.; De Pover, A.; Schoemaker, K.; Fabbro, D.; Gabriel, D.; Simonen, M.; Murphy, L.; Finan, P.; Sellers, W.; Garcia-Echeverria, C. Identification and characterization of NVP-BEZ235, a new orally available dual phosphatidylinositol 3-kinase/mammalian target of rapamycin inhibitor with potent in vivo antitumor activity. *Mol. Cancer Ther.* **2008**, *7*, 1851−1863.
(17) Mukherjee, B.; Tomimatsu, N.; Amancherla, K.; Camacho, C. V.; Pichamoorthy, N.; Burma, S. The dual PI3K/mTOR inhibitor NVP-BEZ235 is a potent inhibitor of ATM- and DNA-PKCs-mediated DNA damage responses. *Neoplasia* **2012**, *14*, 34−43.
(18) Toledo, L. I.; Murga, M.; Zur, R.; Soria, R.; Rodriguez, A.; Martinez, S.; Oyarzabal, J.; Pastor, J.; Bischoff, J. R.; Fernandez-Capetillo, O. A cell-based screen identifies ATR inhibitors with synthetic lethal properties for cancer associated mutations. *Nat. Struct. Mol. Biol.* **2011**, *18*, 721−727.
(19) Foote, K. M.; Nissink, J. W. M. Pyrimidine Indole Derivatives for Treating Cancer. WO2010/073034, 2009.
(20) Miyaura, N.; Yanagi, T.; Suzuki, A. The palladium-catalyzed cross-coupling reaction of phenylboronic acid with haloarenes in the presence of bases. *Synth. Commun.* **1981**, *11*, 513−519.
(21) Ishiyama, T.; Murata, M.; Miyaura, N. Palladium(0)-catalyzed cross-coupling reaction of alkoxydiboron with haloarenes: a direct procedure for arylboronic esters. *J. Org. Chem.* **1995**, *60*, 7508−7510.
(22) Ikenaga, M.; Ishii, Y.; Tada, M.; Kakunaga, T.; Takebe, H. Excision-repair of 4-nitroquinolin-1-oxide damage responsible for killing, mutation, and cancer. *Basic Life Sci.* **1975**, *5B*, 763−771.
(23) Kuntz, I. D.; Chen, K.; Sharp, K. A.; Kollman, P. A. The maximal affinity of ligands. *Proc. Natl. Acad. Sci. U.S.A.* **1999**, *96*, 9997−10002.
(24) Hopkins, A. L.; Lombardo, F.; Alex, A. Ligand efficiency: a useful metric for lead selection. *Drug Discovery Today* **2004**, *9*, 430−431.
(25) Reynolds, C. H.; Bembenek, S. D.; Tounge, B. A. The role of molecular size in ligand efficiency. *Bioorg. Med. Chem. Lett.* **2007**, *17*, 4258−4261.
(26) Tarcsay, A.; Nyiri, K.; Keseru, G. M. Impact of lipophilic efficiency on compound quality. *J. Med. Chem.* **2012**, *55*, 1252−1260.
(27) Allen, F. H. The Cambridge Structural Database: a quarter of a million crystal structures and rising. *Acta Crystallogr.* **2002**, *58*, 380−388.
(28) Bridgland-Taylor, M. H.; Hargreaves, A. C.; Easter, A.; Orme, A.; Henthorn, D. C.; Ding, M.; Davis, A. M.; Small, B. G.; Heapy, C. G.; Abi-Gerges, N.; Persson, F.; Jacobson, I.; Sullivan, M.; Albertson, N.; Hammond, T. G.; Sullivan, E.; Valentin, J.-P.; Pollard, C. E. Optimisation and validation of a medium-throughput electrophysiology-based hERG assay using IonWorks HT. *J. Pharmacol. Toxicol. Methods* **2006**, *54* (2), 189−199.
(29) (a) Kalgutkar, A. S.; Obach, R. S.; Maurer, T. S. Mechanism-based inactivation of cytochrome P450 enzymes: chemical mechanisms, structure−activity relationships and relationship to clinical drug−drug interactions and idiosyncratic adverse drug reactions. *Curr. Drug Metab.* **2007**, *8*, 407−447. (b) Dresser, G. K.; Spence, D.; Bailey, D. G. Pharmacokinetic−pharmacodynamic consequences and clinical relevance of cytochrome P450 3A4 inhibition. *Clin. Pharmacokinet.* **2000**, *38*, 41−57.
(30) Atkinson, A.; Kenny, J. R.; Grime, K. Automated assessment of time-dependent inhibition of human cytochrome P450 enzymes using liquid chromatography-tandem mass spectrometry analysis. *Drug Metab. Dispos.* **2005**, *33*, 1637−1647.
(31) Zimmerlin, A.; Trunzer, M.; Faller, B. CYP3A time-dependent inhibition risk assessment validated with 400 reference drugs. *Drug Metab. Dispos.* **2011**, *39*, 1039−1046.
(32) Zientek, M.; Stoner, C.; Ayscue, R.; Klug-McLeod, J.; Jiang, Y.; West, M.; Collins, C.; Ekins, S. Integrated in silico−in vitro strategy for addressing cytochrome P450 3A4 time-dependent inhibition. *Chem. Res. Toxicol.* **2010**, *23*, 664−676.
(33) Karaman, M. W.; Herrgard, S.; Treiber, D. K.; Gallant, P.; Atteridge, C. E.; Campbell, B. T.; Chan, K. W.; Ciceri, P.; Davis, M. I.; Edeen, P. T.; Faraoni, R.; Floyd, M.; Hunt, J. P.; Lockhart, D. J.; Milanov, Z. V.; Morrison, M. J.; Pallares, G.; Patel, H. K.; Pritchard, S.; Wodicka, L. M.; Zarrinkar, P. P. A quantitative analysis of kinase inhibitor selectivity. *Nat. Biotechnol.* **2008**, *26*, 127−132.
(34) LoVo tumors were selected based on high pan-nuclear γH2AX staining consistent with a high baseline level of replication stress. See the following: Jacq, X.; Smith, L.; Brown, E.; Hughes, A.; Odedra, R.; Heathcote, D.; Barnes, J.; Powell, S.; Maguire, S.; Pearspn, V.; Boros, J.; Caie, P.; Thommes, P.; Nissink, J. W. M.; Foote, K. M.; Jewsbury, P.; Guichard, S. M. AZ20, a Novel Potent and Selective Inhibitor of ATR Kinase with in-Vivo Antitumour Activity. *Proceedings of the 103rd Annual Meeting of the American Association for Cancer Research*, March 31−April 4, 2012; Chicago, IL; AACR: Philadelphia, PA, 2012; *Cancer Res.* **2012**, *72* (8, Suppl.), 1823, DOI: 1538-7445.AM2012-1823.